

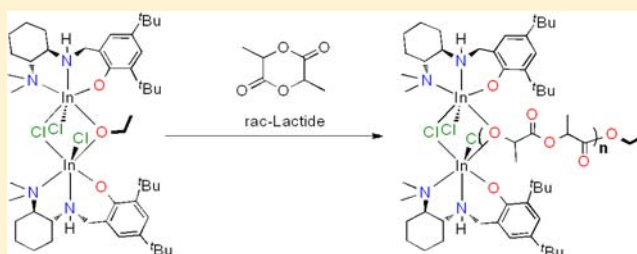
Mechanism of Living Lactide Polymerization by Dinuclear Indium Catalysts and Its Impact on Ioselectivity

Insun Yu, Alberto Acosta-Ramírez, and Parisa Mehrkhodavandi*

Department of Chemistry, University of British Columbia, 2036 Main Mall, Vancouver, BC V6T 1Z1, Canada

S Supporting Information

ABSTRACT: A family of racemic and enantiopure indium complexes **1–11** bearing bulky chiral diaminoaryloxy ligands, $H(NNO_R)$, were synthesized and fully characterized. Investigation of both the mono- and the bis-alkoxy-bridged complexes $[(NNO_R)InX]_2[\mu-Y][\mu-OEt]$ (**5**, $R = tBu$, $X = Y = Cl$; **8**, $R = Me$, $X = I$, $Y = OEt$) by variable temperature, 2D NOESY, and PGSE NMR spectroscopy confirmed dinuclear structures in solution analogous to those obtained by single-crystal X-ray crystallography. The dinuclear complexes in the family were highly active catalysts for the ring-opening polymerization (ROP) of lactide (LA) to form poly(lactic acid) (PLA) at room temperature. In particular, complex **5** showed living polymerization behavior over a large molecular weight range. A detailed investigation of catalyst stereoselectivity showed that, although $(R,R/R,R)$ -**5** is highly selective for *L*-LA, only atactic PLA is obtained in the polymerization of racemic LA. No such selectivity was observed for complex **8**. Importantly, the selectivities obtained for the ROP of racemic LA with $(R,R/R,R)$ -**5** and $(R,R/R,R)$ -**8** are different and, along with kinetics investigations, suggest a dinuclear propagating species for these complexes.



INTRODUCTION

Biodegradable polyesters such as poly(lactic acid) (PLA)¹ have been of intense interest for the past two decades because of their environmental advantages in applications ranging from packaging and agricultural materials to drug delivery and medical devices.² In recent years, the ring-opening polymerization (ROP) of cyclic esters such as lactide (LA) catalyzed by organocatalysts,³ as well as discrete metal complexes bearing various ligand architectures,⁴ has been heavily explored in an attempt to control polymer micro- and macrostructures and limit transesterification or other uncontrolled chain transfer events.⁵ In particular, there has been a strong focus on Lewis acidic centers such as alkali metals,⁶ alkaline earth metals, and Zn,⁷ Al,^{8,9} Ga,¹⁰ Ge,¹¹ Sn,¹² Bi,¹³ Fe,¹⁴ other transition metals,¹⁵ as well as rare earth metals.¹⁶

We are interested in developing catalysts for the controlled ROP of racemic LA (*rac*-LA) and have reported the first example of an indium complex used as an initiator for the living polymerization *rac*-LA¹⁷ to form PLAs with moderate isotactic enrichment and low polydispersity indices (PDIs).¹⁸ We have reported on some properties and applications of these catalysts and the resulting polymers.¹⁹ Following our contributions, other research groups have reported the synthesis of indium complexes supported by both chiral and achiral²⁰ ligands, as well as simple In(III) salts²¹ that were used as lactide polymerization initiators. A number of these indium catalysts are dinuclear^{20b–d} or are postulated to have multinuclear active centers based on model initiators.²¹

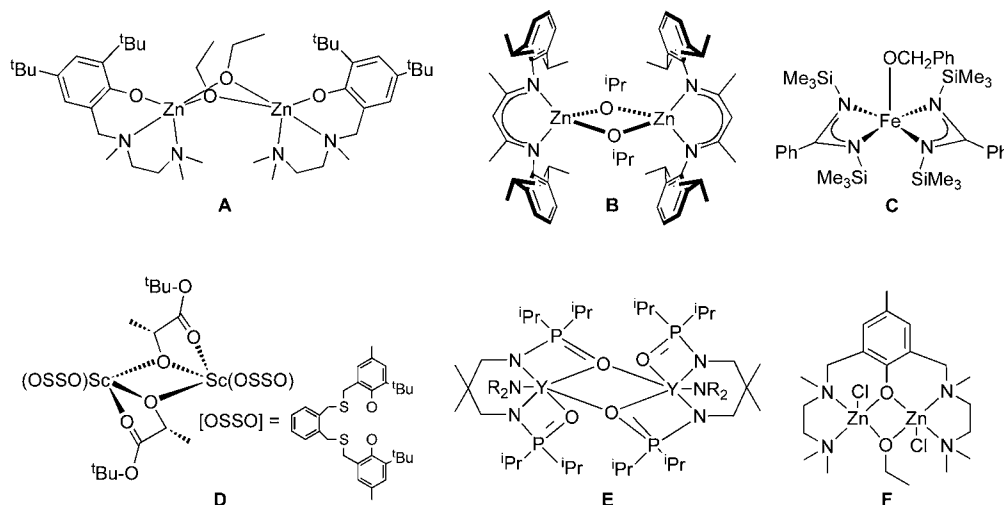
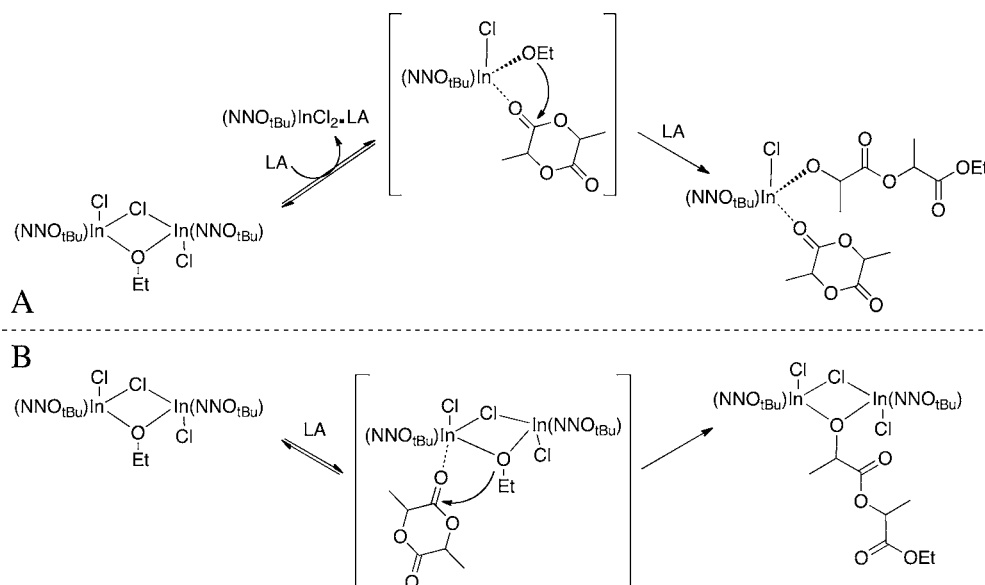
Early reports of catalysts bearing iron,^{22,23} zinc,^{24–26} and rare earth metals^{27,28} demonstrate a range of possibilities for the role

of multiple metal centers in lactide ROP (Scheme 1). One possibility is a catalyst that is dinuclear in the solid state but is mononuclear in solution, as in the case of diaminophenolate zinc alkoxide (**A**).²⁴ In this case, the plot of $-d[LA]/dt$ is proportional to $[A/2]^n$ with $n = 1.33$ (0 °C) or 1.75 (25 °C) indicating a possible fractional dependence on catalyst, although plots of k_{obs} versus $[A/2]_0$ are linear. The dinuclear BDI zinc alkoxide (**B**) complex also exhibits a fractional order in catalyst: $-d[LA]/dt = k_p[Zn]^{1.56}[LA]$.²⁵ A catalyst that is mononuclear in solution as well as in the solid state, such as iron alkoxide catalyst (**C**), can also exhibit fractional order in catalyst.²² This fractional dependence is interpreted by using a model of active chain aggregation.²⁹ In contrast, the scandium complexes bearing 1,ω-dithioalkanediy-bridged bisphenolato (OSSO)-type ligands (**D**) are dinuclear in solution as well as in the solid state.²⁸ A slow dissociation of this dimer to an active lactide adduct **D**/2-lactide similar to those obtained in analogous yttrium complexes was proposed.³⁰ Phosphine oxide-bridged dinuclear yttrium amido complexes (**E**) remain dinuclear in solution as well as in the solid state; however, they can change from a single to a double site catalyst based on the steric bulk of the amido initiator.²⁷ Finally, the dizinc–monoalkoxide complex supported by a dinucleating ligand (**F**) is first order in the dinuclear catalyst and does not show significant aggregation phenomena.²⁶ From the above sample studies, it is clear that significant work is necessary to shed light

Received: May 17, 2012

Published: July 5, 2012

Scheme 1. Some Catalysts for the ROP of Lactide

Scheme 2. Two Mechanistic Proposals for ROP of LA by $[(\text{NNO}_{t\text{Bu}})\text{InCl}]_2(\mu\text{-Cl})(\mu\text{-OEt})$ 

on the subtle mechanistic aspects of polymerization by Lewis acid catalysts capable of aggregation.

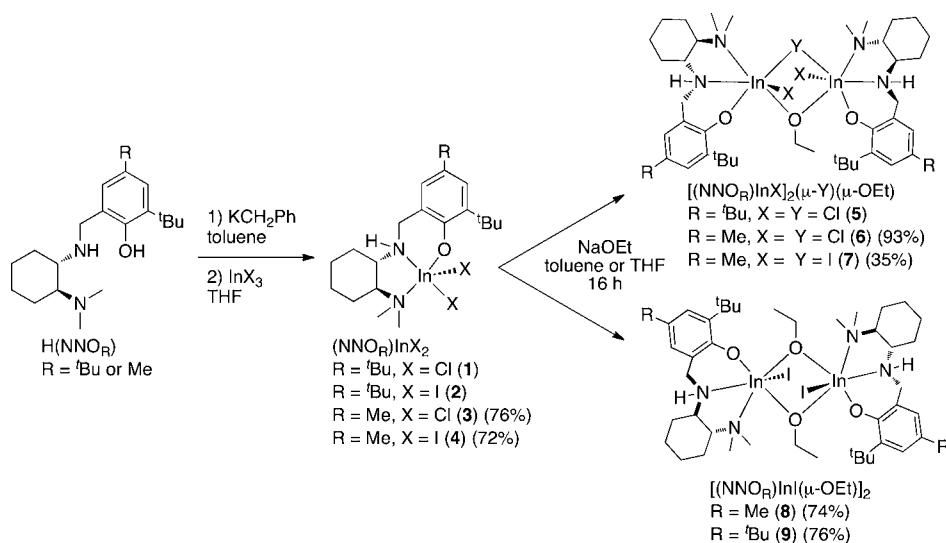
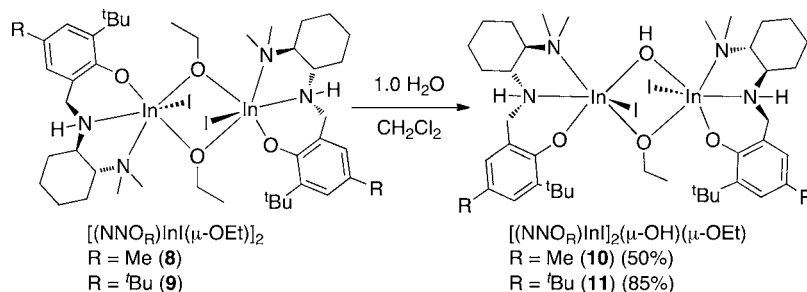
In our initial communication,¹⁷ we reported that an ethoxychloro-bridged dinuclear indium complex, $[(\text{NNO}_{t\text{Bu}})\text{InCl}]_2(\mu\text{-Cl})(\mu\text{-OEt})$, catalyzed the living polymerization of up to 500 equiv of LA following an induction period. We proposed a mechanism similar to that reported for the scandium catalyst **D**, above,^{28,30} involving the dissociation of the dinuclear complex to yield an active mononuclear propagating species $(\text{NNO}_{t\text{Bu}})\text{-In}(\text{Cl})(\text{OEt})$ and an inactive complex $(\text{NNO}_{t\text{Bu}})\text{InCl}_2$ (Scheme 2A).

In this work, we present our full investigation into the polymerization of *rac*-LA by this family of dinuclear alkoxy-bridged catalysts and rule out the dissociative mechanism. Our investigations strongly indicate that the propagating species is dinuclear. We propose an alternative mechanism, involving two metal centers that can stabilize the propagating polymer chain (Scheme 2B), which explains the highly living character of the catalyst. Extensive studies of the stereoselectivity of the catalyst for the ROP of *rac*-, *L*-, and *D*-LA support this mechanism and

provide a more nuanced picture of the various processes involved.

RESULTS

Synthesis and Characterization of Racemic Alkoxy-Bridged Indium Complexes. Racemic 2-*t*-butyl-4-*R*-6-(((2-(dimethylamino)cyclohexyl)amino)methyl)phenol proligands (\pm)- $\text{H}(\text{NNO}_R)$, where *R* is a para methyl or *t*-butyl substituent on the phenol, were synthesized according to previously reported methods (see the Supporting Information).^{17,31} Dihalide indium complexes bearing these ligands, $(\text{NNO}_{t\text{Bu}})\text{-InX}_2$ (**1**, *X* = Cl; **2**, *X* = I) and $(\text{NNO}_{\text{Me}})\text{InX}_2$ (**3**, *X* = Cl; **4**, *X* = I), were prepared by addition of the potassium salts of the proligands, $\text{K}(\text{NNO}_R)$, to the appropriate indium trihalide (Scheme 3, see the Supporting Information for the solid-state structure of (\pm)-**3**).^{19a} Addition of 2 equiv of NaOEt to complexes **1–4** formed monoalkoxy-bridged dinuclear complexes $[(\text{NNO}_{t\text{Bu}})\text{InCl}]_2(\mu\text{-Cl})(\mu\text{-OEt})$ (**5**) and $[(\text{NNO}_{\text{Me}})\text{InX}]_2(\mu\text{-X})(\mu\text{-OEt})$ (*X* = Cl (**6**), I (**7**)). The NMR spectra (CD_2Cl_2) of **6** and **7** prepared from *rac*- $\text{H}(\text{NNO}_{\text{Me}})$ show

Scheme 3. Synthesis of Dinuclear Indium Complexes of the Type $[(\text{NNO}_R)\text{InX}]_2(\mu\text{-Y})(\mu\text{-OEt})$ (**1**, **2**, and **5** Have Been Reported)^{17,19a}Scheme 4. Synthesis of Hydroxy-Bridged Complexes $[(\text{NNO}_R)\text{InI}]_2(\mu\text{-OH})(\mu\text{-OEt})$ 

signals corresponding to one compound, as did the previously reported $[(\text{NNO}_{t\text{Bu}})\text{InCl}]_2(\mu\text{-Cl})(\mu\text{-OEt})$ (**5**) (Figures S5–S8). The solid-state structure of (\pm) -**5** shows a homochiral dimer with $(R,R/R,R)$ centers, implying that the $(S,S/S,S)$ enantiomer also exists in solution.¹⁷

Addition of **4** to a suspension of a 2-fold excess of NaOEt in toluene forms a mixture of **7** and a bis-ethoxy-bridged complex, $[(\text{NNO}_{\text{Me}})\text{InI}(\mu\text{-OEt})]_2$ (**8**), respectively (Scheme 3).³² The analogous, highly insoluble complex with a *para-t*-Bu group, $[(\text{NNO}_{t\text{Bu}})\text{InI}(\mu\text{-OEt})]_2$ (**9**), is synthesized in a similar manner. Upon addition of 1 equiv of water, the bis ethoxy-bridged complexes **8** and **9** convert to the hydroxy-ethoxy dinuclear complexes $[(\text{NNO}_R)\text{InI}]_2(\mu\text{-OH})(\mu\text{-OEt})$ (R = Me (**10**), *t*-Bu (**11**)) (Scheme 4). The ¹H NMR spectra (CD₂Cl₂) of **10** and **11** are similar to the spectra obtained for asymmetrically bridged complexes **5**, **6**, and **7** (Figures S15–18).

The molecular structure of **9**, which was synthesized from *rac*-H(NNO_{*t*Bu}), shows a heterochiral dimer (*meso*-**9**) with $(R,R/S,S)$ configuration (Figure 1). In contrast, the solid-state structure of **11**, synthesized from *rac*-H(NNO_{*t*Bu}), shows a homochiral dimer with $(R,R/R,R)$ configuration, implying that the $(S,S/S,S)$ analogue of (\pm) -**11** exists in solution (Figure 2). Complexes **5** and **11** have similar In–N bond distances, and there is a “cis” relationship between the phenoxy moieties of the ligand (the phenoxy groups are on the same hemisphere of the molecule). Addition of excess water to these complexes forms the previously described hydroxy-bridged complexes $[(\text{NNO}_R)\text{InX}(\mu\text{-OH})]_2$.^{19a}

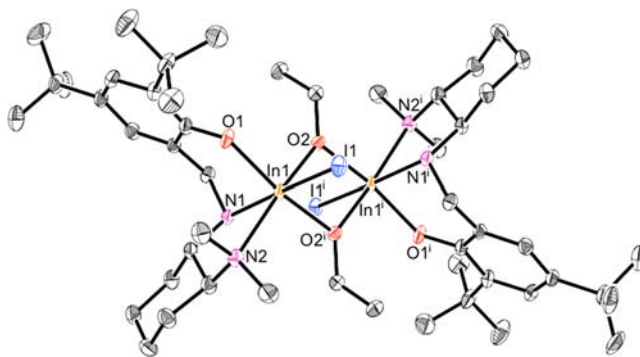


Figure 1. Molecular structure of *meso*-**9** (depicted with ellipsoids at 50% probability and H atoms omitted for clarity). Selected bond lengths (Å): In1–I1 2.8068(3), In1–O1 2.082(2), In1–O2 2.163(2), In1–N1 2.275(2), In1–N2 2.381(3). Selected bond angles (deg): O1–In1–O2ⁱ 91.22(8), O1–In1–O2 163.88(8), O1–In1–I1 92.77(6), O1–In1–N1 85.06(8), O1–In1–N2 94.93(9), N1–In1–N2 75.97(9), N2–In1–O2 98.69(9), Ni–In1–I1 171.11(6), In1–O2–In1ⁱ 105.84(8).

Synthesis and Characterization of Enantiopure Alkoxy-Bridged Indium Complexes. (R,R) - and (S,S) -H(NNO_R), where R is a *para*-methyl or *t*-butyl substituent on the phenol group, were synthesized in a manner analogous to that of (\pm) -H(NNO_R) (see the Supporting Information),^{17,31} as were the dihalide complexes $(\text{NNO}_{t\text{Bu}})\text{InX}_2$ ((R,R) - and (S,S) -**1**: X = Cl) and $(\text{NNO}_{\text{Me}})\text{InX}_2$ ((R,R) - and (S,S) -**4**: X =

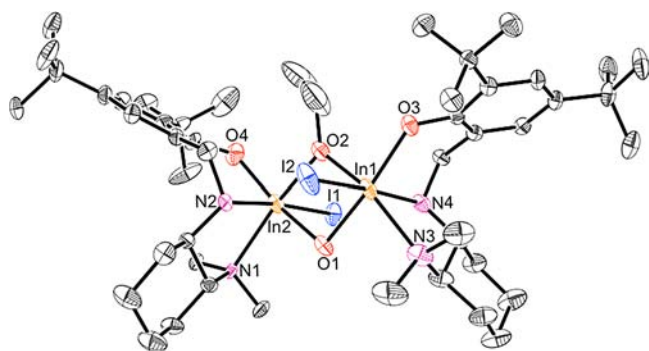


Figure 2. Molecular structure of (\pm)-**11** (depicted with ellipsoids at 50% probability and H atoms as well as solvent molecules omitted for clarity). Selected bond lengths (Å): In1–O1 2.180(3), In2–O1 2.211(3), In1–O2 2.142(3), In2–O2 2.146(3), In1–O3 2.090(3), In1–N3 2.336(4), In1–N4 2.273(4), In1–I2 2.8030(4), In2–I1 2.7923(4), In2–O4 2.099(5), In2–N1 2.338(9), In2–N2 2.265(5). Selected bond angles (deg): O1–In1–O2 92.49(12), N3–In1–I2 96.20(10), N3–In1–O3 103.29(14), N1–In2–I1 98.20(15), N1–In2–O4 100.14(5), O1–In2–O2 74.58(12), In1–O1–In2 103.26(13), In1–O2–In2 106.90(14), O2–In1–O3 165.62(12).

1). The NMR spectra of the enantiomers are identical to those of the racemic complexes (see the Supporting Information). The solid-state structure of (*S,S*)-**4** shows a distorted trigonal bipyramid with the iodo ligands in the axial and equatorial positions, while in (\pm)-**3** both chloro ligands are in the equatorial position (Figures S22 and S23).

Enantiopure mono- and bis-ethoxy-bridged complexes (*R,R,S,S*-**5**) and (*R,R,S,S*)-**8**) were synthesized in a manner analogous to that of their racemic counterparts. The ^1H NMR spectra of complex **5** generated from (\pm)-, (*R,R*)-, and (*S,S*)- $\text{H}(\text{NNO}_{\text{Et}})$ are identical, suggesting that the species observed in solution for (\pm)-**5** are indeed the two homochiral enantiomers (*R,R/R,R*)- and (*S,S/S,S*)-**5** (Figure 3a). In contrast, while the ^1H NMR spectra of (*R,R/R,R*)- and (*S,S/S,S*)-**8** are identical, the ^1H NMR spectrum of *meso*-**8** is different and shows only two signals for each of $\text{Ar}-\text{CH}_2-\text{N}$

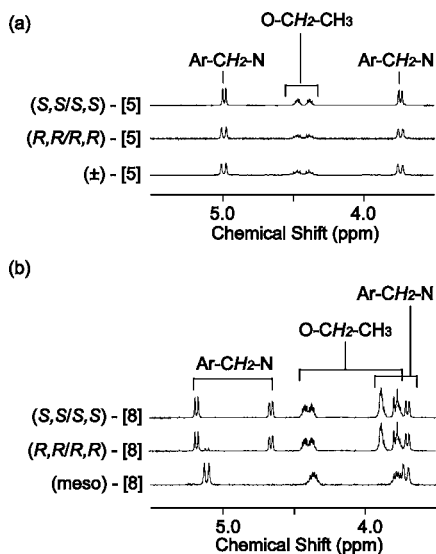


Figure 3. ^1H spectra (CDCl_3 , 25 °C) of (a) (\pm)-, (*R,R/R,R*)-, and (*S,S/S,S*)-**5**, and (b) (*meso*)-, (*R,R/R,R*)-, and (*S,S/S,S*)-**8**.

and $\text{O}-\text{CH}_2\text{CH}_3$, as would be expected from a centrosymmetric complex (Figure 3b).

The molecular structure of (*S,S/S,S*)-**8**, obtained by single-crystal X-ray diffraction, shows two homochiral octahedral indium centers with no center of symmetry in the molecule (Figure 4). This is in contrast to the structure of *meso*-**9** (Figure

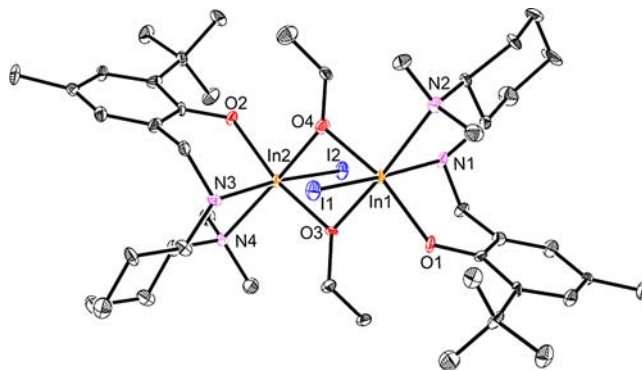


Figure 4. Molecular structure of (*S,S/S,S*)-**8** (depicted with ellipsoids at 50% probability and H atoms omitted for clarity). Selected bond lengths (Å): In1–O1 2.101(4), In2–O2 2.100(4), In1–O3 2.187(4), In2–O3 2.174(3), In1–O4 2.176(3), In2–O4 2.174(4), In1–N1 2.270(5), In1–N2 2.387(5), In2–N3 2.259(5), In2–I4 2.379(4), In1–I1 2.8052(5), In2–I2 2.7980(5). Selected bond angles (deg): O1–In1–O4 162.29(15), O1–In1–O3 87.89(14), O4–In1–O3 75.07(11), O1–In1–N1 85.27(16), O4–In1–N1 92.39(16), O3–In1–N1 98.38(17), O1–In1–N2 98.69(14), O4–In1–N2 97.80(14), O3–In1–N2 171.12(15), N1–In1–N2 76.36(18), O1–In1–I1 92.23(12), O4–In1–I1 93.22(12), O3–In1–I1 92.35(11), N1–In1–I1 168.87(12), N2–In1–I1 93.35(13), O2–In2–O4 88.28(14), O2–In2–O3 163.08(14), O4–In2–O3 75.38(11), O2–In2–N3 89.10(16), O4–In2–N3 95.78(16), O3–In2–N3 88.24(15), O2–In2–N4 92.31(14), O4–In2–N4 172.58(17), O3–In2–N4 103.33(14), N3–In2–N4 76.84(16), O2–In2–I2 93.25(12), O4–In2–I2 92.14(12), O3–In2–I2 91.74(11), N3–In2–I2 171.81(11), N4–In2–I2 95.22(12).

1) that shows a centrosymmetric heterochiral dimer. *meso*-**8** is the thermodynamically favored form of the complex: a 1:1 mixture of (*R,R/R,R*)- and (*S,S/S,S*)-**8** converts to (*R,R/S,S*)-**8** in a few hours at room temperature (Figure S21). Reaction of (*R,R/R,R*)-**8** with adventitious water forms the nearly isostructural bis-hydroxy-bridged complex (*R,R/R,R*)- $[(\text{NNO}_{\text{Me}})\text{In}(\text{I})(\mu\text{-OH})]_2$ (Figure S24). Again, this is in contrast to the bis-hydroxy-bridged dimers in this series, which have been isolated in the centrosymmetric *meso*-forms.^{17,19a}

Dinuclear Nature of Ethoxy-Bridged Complexes in Solution. All alkoxy-containing complexes in this family have a dinuclear structure in the solid state, and we show above that the solution structures of (*S,S/S,S*)- and (*R,R/S,S*)-**8** reflect the differences observed in the analogous solid-state structures. Additional data, below, support the dinuclear nature of the alkoxy-bridged complexes in solution.

- (1) Variable-temperature ^1H NMR spectra of **5** and **8** show no changes over a wide temperature range (Figures S25 and S26).
- (2) NOE experiments with **5** and **8** support dinuclear structures. The ^1H NOESY-2D NMR spectrum of **5** shows through-space interactions between $\text{In}-\text{OCH}_2\text{CH}_3$ and the phenolate *ortho*- $\text{C}(\text{CH}_3)_3$ protons only (Figure S27). Importantly, cross peaks are not

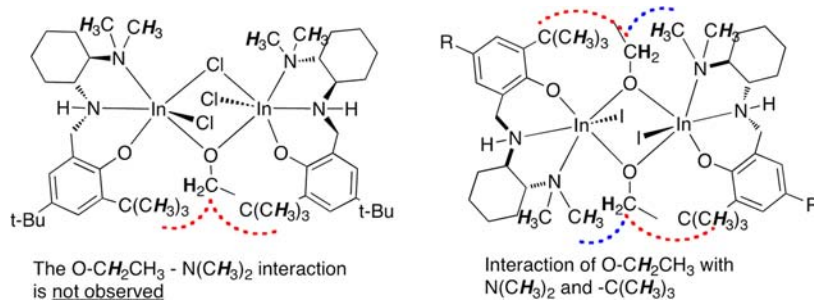


Figure 5. Through-space interactions expected for mononuclear ethoxy complexes and observed in the ^1H NOESY-2D NMR spectra of complexes **5** (left), and **8** and **9** (right) (CDCl_3 , 25°C).

observed between $\text{In}-\text{OCH}_2\text{CH}_3$ and the protons of $\text{N}(\text{CH}_3)_2$, indicating an asymmetric environment around $\text{In}-\text{OCH}_2\text{CH}_3$ (Figure 5, left). There is also a clear through-space interaction between $\text{In}-\text{OCH}_2\text{CH}_3$ and only one of the NCH_2-Ar protons of the ancillary ligand. In contrast, the ^1H NOESY-2D NMR spectrum of **8** (Figure 5 right) shows through-space interactions between OCH_2CH_3 and the phenolate *ortho*- $\text{C}(\text{CH}_3)_3$ as well as between $\text{In}-\text{OCH}_2\text{CH}_3$ and the protons of $\text{N}(\text{CH}_3)_2$ (Figure S28). Similar cross peaks are observed for complex **9** (Figure S29). The calculated distances between $\text{In}-\text{OCH}_2\text{CH}_3$ and ligand protons for **5** and **8** using ^1H NOESY-1D spectroscopy are in good agreement with the values obtained from the solid-state structures (Figures S30 and S31).

- (3) Pulsed-gradient spin-echo (PGSE) NMR experiments³³ are in agreement with the solid-state structures and support dinuclear solution structures for **5** and **8**. The diffusion coefficients (D_t) of the proligand ($12.0 \times 10^{-10} \text{ m}^2 \text{ s}^{-1}$), the mononuclear complex **1** ($10.4 \times 10^{-10} \text{ m}^2 \text{ s}^{-1}$), and the previously reported complex $(\text{NNO}_{\text{tBu}})\text{In}(\text{CH}_3)_2$ ($11.1 \times 10^{-10} \text{ m}^2 \text{ s}^{-1}$)^{19a} are significantly faster than those of **5** ($7.8 \times 10^{-10} \text{ m}^2 \text{ s}^{-1}$) and **8** ($7.9 \times 10^{-10} \text{ m}^2 \text{ s}^{-1}$) (Figure S32). The hydrodynamic radii (r_H) of the dinuclear species (**5**, 7.5 \AA ; **8**, 7.4 \AA) calculated from the modified Stokes-Einstein equation³³ are consistent with the structurally determined values (**5**, 7.3 \AA ; **8**, 6.7 \AA) estimated from the X-ray crystallographic data (Table S4).

Living Ring-Opening Polymerization (ROP) of Lactide.

Dinuclear complexes **5**, **7**, **8**, and **10** are excellent initiators for lactide polymerization and were studied in depth. The choice of solvent for carrying out comparative experiments was complicated by the limited solubility of the bis-ethoxy-bridged complex **8** in all solvents except CDCl_3 ; the role of solvent will be discussed further below.

The rates of LA ROP with the *para*-*t*-Bu and -Me substituted complexes **5** and **6** are identical under the same conditions (Figure S33). The reactions of *rac*-LA with catalysts **5**, **6**, **8**, and **10** were monitored by ^1H NMR spectroscopy at 25°C up to 90% conversion of 200 equiv of *rac*-LA (~ 50 min), with variations in rate depending on the initiator and reaction conditions. In all cases, an induction period was observed (Figure S34).

After the initiation period, the polymerization rates are first order in LA concentration ($\text{rate} = k_{\text{obs}}[\text{LA}]$). The polymerization rate is also first order in the concentration of dinuclear complexes **5**, **7**, **8**, and **10**, indicating that there is one initiating species for all complexes, and give an overall second-order rate

law ($\text{rate} = k[\text{catalyst}][\text{LA}]$) (Figure S35). This allows us to directly compare k values for the four catalysts in question (Table 1).

Table 1. Rate Constants for the ROP of *rac*-LA Using Dinuclear Indium Initiators^a

entry	catalyst	k ($\text{M}^{-1} \text{ s}^{-1}$)
1 ^b	$[(\text{NNO}_{\text{tBu}})\text{InCl}]_2(\mu\text{-OEt})(\mu\text{-Cl})$ (5)	0.57(0.05)
2 ^b	$[(\text{NNO}_{\text{Me}})\text{InI}]_2(\mu\text{-OEt})(\mu\text{-I})$ (7)	1.35(0.11)
3 ^c	$[(\text{NNO}_{\text{Me}})\text{InI}(\mu\text{-OEt})]_2$ (8)	1.78(0.26)
4 ^b	$[(\text{NNO}_{\text{Me}})\text{InI}]_2(\mu\text{-OEt})(\mu\text{-OH})$ (10)	1.50(0.13)

^aAll reactions were carried out in an NMR tube in CDCl_3 at 25°C and followed by 90% conversion. ^b $[\text{LA}] = 0.91 \text{ M}$. $[\text{catalyst}] = 0.0091 \text{ M}$. ^c $[\text{LA}] = 0.228 \text{ M}$. $[\text{catalyst}] = 0.00228 \text{ M}$. 1,3,5-Trimethoxybenzene (TMB) was used as internal standard. The value of k_{obs} was determined from the slope of the plots of $\ln([\text{LA}]/[\text{TMB}])$ versus time.

The rate constant for the ROP of LA with **5** in CDCl_3 is comparable to the reported value in CD_2Cl_2 .¹⁷ The rates of propagation for the iodo analogues, **7**, **8**, and **10**, are significantly higher than that for **5**. On the basis of our previous studies on the role of halides in dinuclear indium complexes,^{19a} we believe that this increase is due to the greater electrophilicity of the indium centers in the chloro analogues. This enhanced electrophilicity is expected to strengthen the initiator-LA interaction and slow ring-opening and propagation. Importantly, the monoalkoxy complexes **7** and **10** have nearly identical rates, within error, to the bis-alkoxy-bridged complex **8** (Table 1, entries 2–4). This would not be expected if complex **8** dissociated to form two initiating species. The activation parameters of the mono- and bis-ethoxy-bridged complexes **7** ($\Delta H^\ddagger = 47(3) \text{ kJ mol}^{-1}$, $\Delta S^\ddagger = -83(7) \text{ J K}^{-1} \text{ mol}^{-1}$) and **8** ($\Delta H^\ddagger = 62(4) \text{ kJ mol}^{-1}$, $\Delta S^\ddagger = -30(3) \text{ J K}^{-1} \text{ mol}^{-1}$)³⁴ are in agreement with reported values for complex **5** and other indium catalysts for LA ROP and indicate similar ordered transition states in a coordination-insertion mechanism (Figures S36, S37).^{17,20b}

In our communication,¹⁷ we reported that the ROP of LA with **5** was a living process, with a linear increase of M_n values and low molecular weight distributions for monomer:initiator (M/I) ratios up to 500. We have expanded this range to M/I ratios of over 2100 with the same control, obtaining polymers with molecular weights up to 350 kDa with very low PDI values (Figure 6). These results confirm that complex **5** is one of the most controlled catalysts reported for the ROP of LA.^{4,5}

Although the rates of polymerization for the mono- and bis-ethoxy-bridged complexes **7** and **8** are identical, the molecular

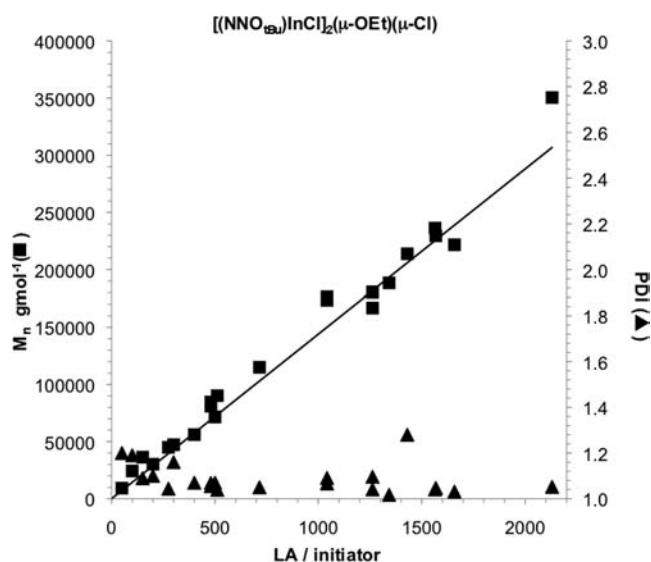


Figure 6. Plot of observed PLA M_n (■) and molecular weight distribution (▲) as functions of added *rac*- or *L*-LA for catalyst **5** (M_n = number averaged molecular weight, PDI = polydispersity index). The line indicates calculated M_n values based on the LA: initiator ratio. All reactions were carried out at room temperature in CH_2Cl_2 , and polymer samples were obtained at >90% conversion.

weight of polymers obtained using the two catalysts depends on the number of alkoxides in the molecule (Table 2). Polymers obtained with the monoethoxy-bridged catalysts **5** and **7** show a good correlation between the theoretical M_n based on dimer concentration (Table 2, entries 1–4). In contrast, those obtained with the bis-ethoxy-bridged complex **8** show M_n values roughly one-half of the theoretical values, indicating the presence of two propagation sites for **8** (Table 2, entries 5–7). Thus, for the bis-ethoxy-bridged catalyst **8**, polymer molecular weights are indicative of one polymer chain per ethoxide.

Control of Stereoselectivity with Dinuclear Catalysts.

We have previously communicated that (\pm) -**5** exerts moderate isoselectivity for the ROP of *rac*-LA ($P_m = 0.62$).¹⁷ In the current study, we investigate the stereoselectivity of racemic and enantiopure dinuclear complexes (\pm) -, (*R,R/R,R*)-, and (*S,S/S,S*)-**5** and *meso*-, (*R,R/R,R*)-, and (*S,S/S,S*)-**8** for the polymerization of *rac*-, *D*-, and *L*-LA (CDCl_3 , 25 °C) in depth (Figures S38–S41). We do not observe a halide effect: selectivities for (\pm) - $[(\text{NNO}_{\text{tBu}})\text{InCl}]_2(\mu\text{-OEt})(\mu\text{-Cl})$ (**5**) and

(\pm) - $[(\text{NNO}_{\text{Me}})\text{InI}]_2(\mu\text{-OEt})(\mu\text{-I})$ (**7**) are identical (Figure S40g).

The rates of polymerization for enantiopure **5** reveal strong site selectivity. Comparison of the ROP rates for *D*- and *L*-LA with (*R,R/R,R*)-**5** shows a k_L/k_D value of ~ 14 ; the reverse value ($k_D/k_L \approx 14$) is obtained for (*S,S/S,S*)-**5** (Table 3, entries 1–

Table 3. Effects of Catalyst Chirality on Reaction Rates and Polymer Tacticity by Mono-ethoxy-Bridged Complex **5**^a

entry	catalyst	monomer	k_{obs} ($\times 10^{-3} \text{ s}^{-1}$) ^b	P_m
1	(<i>R,R/R,R</i>)- 5	<i>L</i> -LA	3.4 (0.6)	1
2	(<i>R,R/R,R</i>)- 5	<i>D</i> -LA	0.25 (0.14)	1
3	(<i>S,S/S,S</i>)- 5	<i>L</i> -LA	0.27 (0.04)	1
4	(<i>S,S/S,S</i>)- 5	<i>D</i> -LA	3.8 (0.8)	1
5	(<i>R,R/R,R</i>)- 5	<i>rac</i> -LA	0.62 (0.16) ^c 0.21 (0.06) ^d	0.48
6	(<i>S,S/S,S</i>)- 5	<i>rac</i> -LA	0.70 (0.05) ^c 0.24 (0.01) ^d	0.49
7	(\pm) - 5	<i>L</i> -LA	2.98 (0.09)	1
8	(\pm) - 5	<i>D</i> -LA	2.95 (0.08)	1
9	(\pm) - 5	<i>rac</i> -LA	1.72 (0.16)	0.61

^aAll reactions were carried out with 200 equiv of LA in CDCl_3 at 25 °C and followed to 90% conversion by ¹H NMR spectroscopy, unless otherwise stated. [catalyst] = 0.0023 M, [LA] = 0.45 M. ^bAverage of two experiments. ^c k_{obs} from 0% to 64% conversion. ^d k_{obs} from 73% to 90% conversion.

4).³⁶ This k_{rel} value is similar to those reported for highly selective chiral aluminum salen complexes.⁹ Despite this high selectivity, and in contrast to the aluminum systems, polymerization of *rac*-LA with enantiopure **5** forms atactic PLA (Table 3, entries 5,6). Polymerization of *rac*-LA with (*R,R/R,R*)-**5** follows two rate regimes (Figure 7a). In the early stages of the polymerization, a rate of $0.62 \times 10^{-3} \text{ s}^{-1}$ is observed; however, after ~ 30 min, there is a sharp decrease in the rate to $0.21 \times 10^{-3} \text{ s}^{-1}$. This is the rate observed for the disfavored monomer. Similar values are observed for (*S,S/S,S*)-**5**, indicating that the favored monomer is polymerized first, at a faster rate, than the disfavored (Figure S38). In contrast, the k_{obs} values for polymerization of *L*- and *D*-LA with (\pm) -**5** (Table 3, entries 7,8) are identical to the analogous enantiopure complexes within error (Table 3, entries 1,4). Importantly, the rate of polymerization of *rac*-LA with (\pm) -**5** (Table 3, entry 1) is significantly lower than the rates for enantiopure monomers, indicating catalyst inhibition by the mismatched monomer.

There is a nonlinear relationship between the observed rate constant and percent (*R,R/R,R*)-**5**. As the enantiopurity of the

Table 2. Polymerization *rac*-LA by Complexes **5**, **7**, and **8**

entry	initiator	$[\text{LA}]_0$: [dimer]	solvent	conv. ^a (%)	$M_{n,\text{theo}}$ ^b /g mol ⁻¹	$M_{n,\text{GPC}}$ ^c /g mol ⁻¹	M_w/M_n ^c
1	5	1005	CH_2Cl_2	93	134 760	129 800	1.04
2	5	1002	CHCl_3	98	141 580	148 400	1.04
3	7	510	CH_2Cl_2	95	68 880	50 050	1.17
4	7	976	CH_2Cl_2	95	133 680	141 700	1.12
5	8	500	CH_2Cl_2	92	66 350	35 940	1.16
6	8	1000	CH_2Cl_2	93	134 090	61 490	1.14
7	8	2001	CH_2Cl_2	95	273 960	154 900	1.26

^aMonomer conversion, determined by ¹H NMR spectroscopy. ^bCalculated from $[\text{LA}]_0/[\text{initiator}] \times \text{LA conversion} \times M_{\text{LA}} + M_{\text{EtOH}}$. ^cDetermined by GPC–LALLS (gel permeation chromatography–low angle laser light scattering) to the polystyrene standard calibration curve via the Mark–Houwink equation in THF at 25 °C ($[\eta] = KM^a$, while $[\eta]$ = intrinsic viscosity, M = molecular weight, and K and a are Mark–Houwink parameters, $K = 1.832 \times 10^{-4} \text{ dL/g}$, and $a = 0.69 \text{ dn/dc} = 0.042 \text{ mL/g}$).³⁵ All reactions were carried out for 16 h.

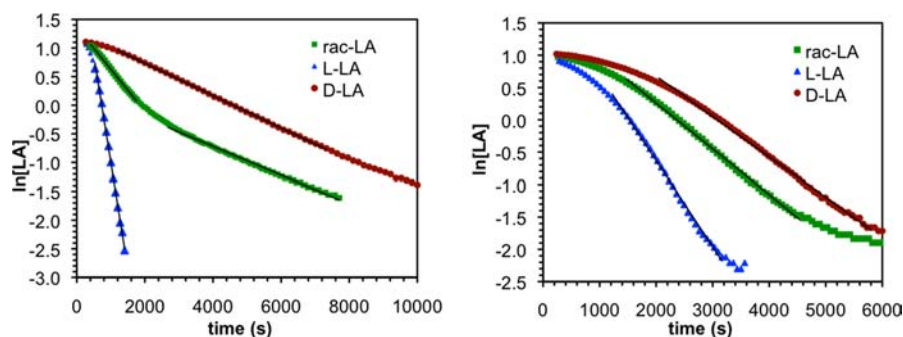


Figure 7. Plot of $\ln[\text{LA}]$ versus time for polymerization of *rac*-LA, L-LA, and D-LA by (a, left) (R,R/R,R)-5 and (b, right) (R,R/R,R)-8 (CDCl_3 , 25 °C).

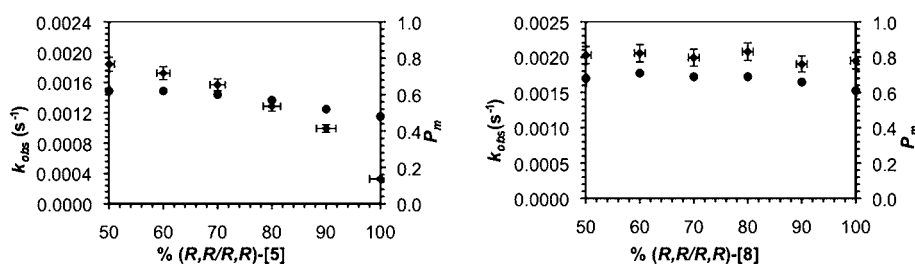


Figure 8. Plots of k_{obs} (◆) and P_m (●) as functions of catalyst enantiopurity. All reactions were carried out with 200 equiv of *rac*-LA in CDCl_3 at 25 °C and followed to 90% conversion. (a, left) [5] = 0.0024 M, [LA] = 0.46 M; (b, right) [8] = 0.00057 M, $[\text{LA}] = 0.117$ M.

samples increases from (\pm)-5 (50%) to (R,R/R,R)-5 (100%), the observed rate constants decrease an order of magnitude in a nonlinear fashion, while P_m values decrease from ~ 0.6 to 0.5, again in a nonlinear fashion (Figure 8a). Such nonlinear relationships are a characteristic of dinuclear stereoselective catalysts.³⁷ P_m values for ROP of *rac*-LA with (\pm)- and (R,R/R,R)-5 remain essentially unchanged with increasing conversion (at 25 and 0 °C), confirming that the resulting polymers are not blocky (Figure S41).

In contrast to the monoethoxy-bridged complex 5, polymerizations of LA with bis-ethoxy-bridged complex 8 does not show significant site selectivity. The k_L/k_D value for ROP of L-LA with (R,R/R,R)-8 is only ~ 2 , with the opposite selectivity of the same magnitude observed for (S,S/S,S)-8 (Table 4, entries 1–4). P_m values for the polymerizations of *rac*-LA with *meso*- or enantiopure 8 are the same (Table 4, entries 5–7). The rate constants for ROP of *rac*-, D-, and L-LA with *meso*-8 are identical within experimental error (Table 4, entries 7–9).

Table 4. Effects of Catalyst Chirality on Reaction Rates and Polymer Tacticity by Bis-ethoxy-Bridged Complex 8^a

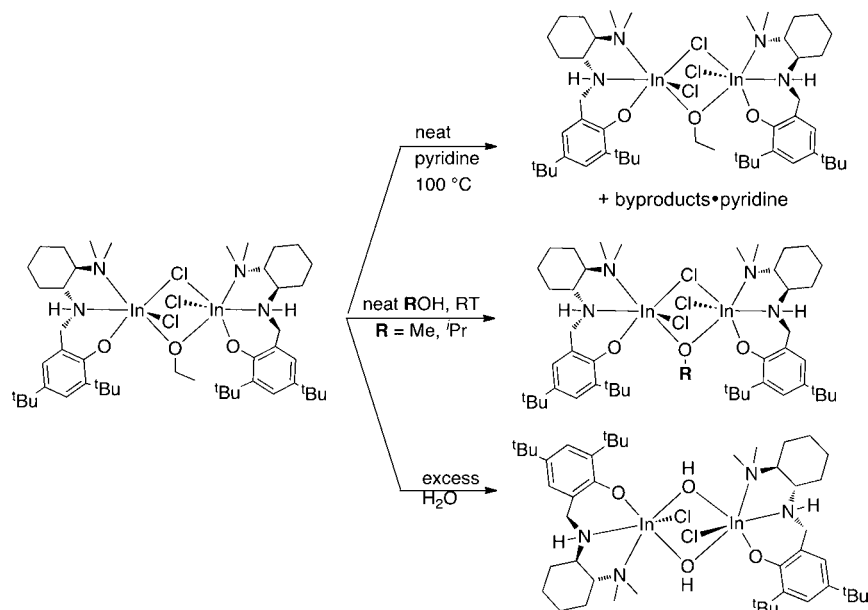
entry	catalyst	monomer	$k_{\text{obs}} (\times 10^{-3} \text{ s}^{-1})^b$	P_m
1	(R,R/R,R)-[8]	L-LA	1.25 (0.21)	1
2	(R,R/R,R)-[8]	D-LA	0.64 (0.01)	1
3	(S,S/S,S)-[8]	L-LA	0.67 (0.16)	1
4	(S,S/S,S)-[8]	D-LA	1.29 (0.30)	1
5	(R,R/R,R)-[8]	<i>rac</i> -LA	0.72 (0.01)	0.65
6	(S,S/S,S)-[8]	<i>rac</i> -LA	0.66 (0.09)	0.64
7	(<i>meso</i>)-[8]	<i>rac</i> -LA	1.73 (0.76)	0.62
8	(<i>meso</i>)-[8]	L-LA	1.24 (0.03)	1
9	(<i>meso</i>)-[8]	D-LA	1.23 (0.02)	1

^aAll reactions were carried out with 200 equiv of LA in CDCl_3 at 25 °C and followed to 90% conversion by ¹H NMR spectroscopy. [catalyst] = 0.00052 M, [LA] = 0.114 M. ^bAverage of two experiments.

Observed rate constants and P_m values do not change with increasing enantiopurity of the catalyst (Figure 8b). These data suggest that the observed selectivity ($P_m = 0.65$) with catalyst 8 is not affected by catalyst chirality and thus must be dominated by chain end control.

On the Solution Structure of the Propagating Species for Catalyst 5. The P_m values obtained for the ROP of *rac*-LA with (R,R/R,R)-5 (0.48) and (R,R/R,R)-8 (0.65) are significantly different. This would not be possible if the polymers were derived from identical mononuclear initiators. Indeed, the kinetics and selectivity data discussed above strongly suggest a dinuclear propagating species for catalyst 5.

To probe the nature of the catalyst during polymerization and differentiate between the mechanisms outlined in Scheme 2, we monitored the dissociation of 5 in the presence of added donors. Complex 5 remains unchanged after 24 h after the addition of 2 equiv of pyridine, ethyl acetate, and ethanol, as observed by ¹H NMR spectroscopy (CDCl_3 , 25 °C, Figure S42). Irreversible changes are observed upon addition of a larger excess of a donor (Scheme 5). Variable-temperature ¹H NMR spectra (25 to -82 °C, CD_2Cl_2) of a mixture of 5 and 10 equiv of pyridine show new signals for coordinated pyridine, which can be observed below -30 °C (Figure S43). When complex 5 is heated to 100 °C in neat pyridine for 48 h, signals for at least two new complexes as well as pyridine are observed in the ¹H NMR spectra; however, complex 5 remains the major species in solution (Figure S44). A 2D NOESY spectrum of this mixture shows no correlations between the proton signals of pyridine and 5, while correlations between pyridine and at least one of the new byproducts are observed (Figure S45). We have reported that in a similar reaction with $[\text{NNO}_{\text{tBu}}]\text{InCl}_2$ (1), the pyridine adduct forms quantitatively.¹⁷ Therefore, dinuclear complex 5 may be dissociated in the presence of a strong base under forcing conditions to form base-adducts; however, the majority of the parent complex 5 remains

Scheme 5. Irreversible Reactions of $[(\text{NNO}_{t\text{Bu}})\text{InCl}]_2(\mu\text{-Cl})(\mu\text{-OEt})$ (**5**) with Donors

unreacted, attesting to the stability of the dinuclear structure in solution.

The thermodynamic stability of the dinuclear complex does not preclude reactivity. As previously reported, reaction of (\pm)-**5** with water yields the *meso* form of the bis-hydroxy-bridged complex $(R,R/S,S)-[(\text{NNO}_{t\text{Bu}})\text{In}(\text{Cl})(\mu\text{-OH})]_2$.^{17,19a} The *meso* complex can only be formed if the $(R,R/R,R)$ - and $(S,S/S,S)$ -**5** dissociate during the reaction. Also, when **5** is dissolved in neat methanol or isopropanol at room temperature, the NMR spectra of the resulting products show resonances corresponding to the quantitative formation of new metal methoxide and isopropoxide complexes (Figure S46). Integration of the ¹H NMR spectra of these new species clearly shows that the complexes maintain a monoalkoxy-bridged dinuclear structure analogous to complex **5**.

The reactivity with alcohols and water shows that dinuclear complexes such as **5** are undergoing some dissociation in the presence of added species. Indeed, cross over reactions between (\pm)- $[(\text{NNO}_{t\text{Bu}})\text{InCl}]_2(\mu\text{-Cl})(\mu\text{-OEt})$ (**5**) and $(\text{NNO}_{\text{Me}})\text{InCl}_2$ (**3**), as well as $[(\text{NNO}_{\text{Me}})\text{In}]_2(\mu\text{-I})(\mu\text{-OEt})$ (**7**) and the $(\text{NNO}_{t\text{Bu}})\text{InI}_2$ (**2**), are observed in 5 min (Figures S47, S48). A similar crossover reaction was observed between *meso*- $[(\text{NNO}_{\text{Me}})\text{In}(\text{I})(\mu\text{-OEt})]_2$ (*meso*-**8**) and (\pm)- $(\text{NNO}_{t\text{Bu}})\text{InI}_2$ (**2**) (Figure S49).

The potential lability of the dinuclear catalysts is not a factor in lactide polymerization. If the dinuclear complex **5** is dormant and dissociation to an active mononuclear species is required for polymerization (Scheme 2a), addition of $[(\text{NNO}_{t\text{Bu}})\text{InCl}]_2$ (**1**) should shift the equilibrium toward the unreactive species and affect polymerization rates and/or polymer molecular weights. In a series of experiments, different amounts of **1** were added to a solution of **5** (CD_2Cl_2 , 25 °C) prior to the addition of monomer to the catalyst mixture, and the polymerization was monitored by ¹H NMR spectroscopy. In an identical set of reactions, the polymer was isolated and analyzed. The resulting values of k_{obs} and M_n remain constant with up to 5 additional equiv of **1** (Figure 9). At higher concentrations of **1**, the solution becomes saturated. These experiments indicate that, although complex **5** can dissociate in the presence of donors,

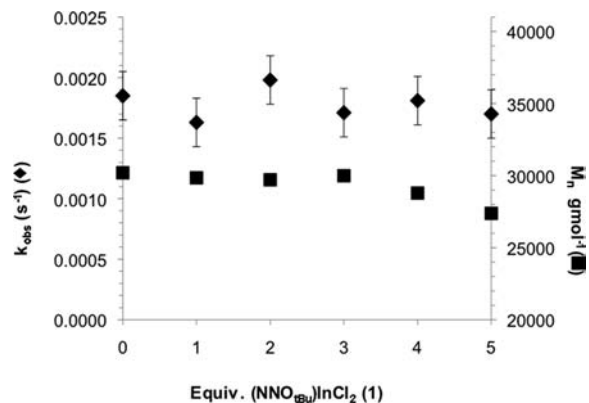
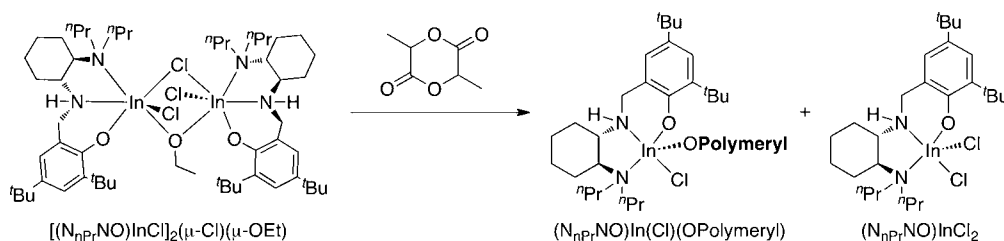
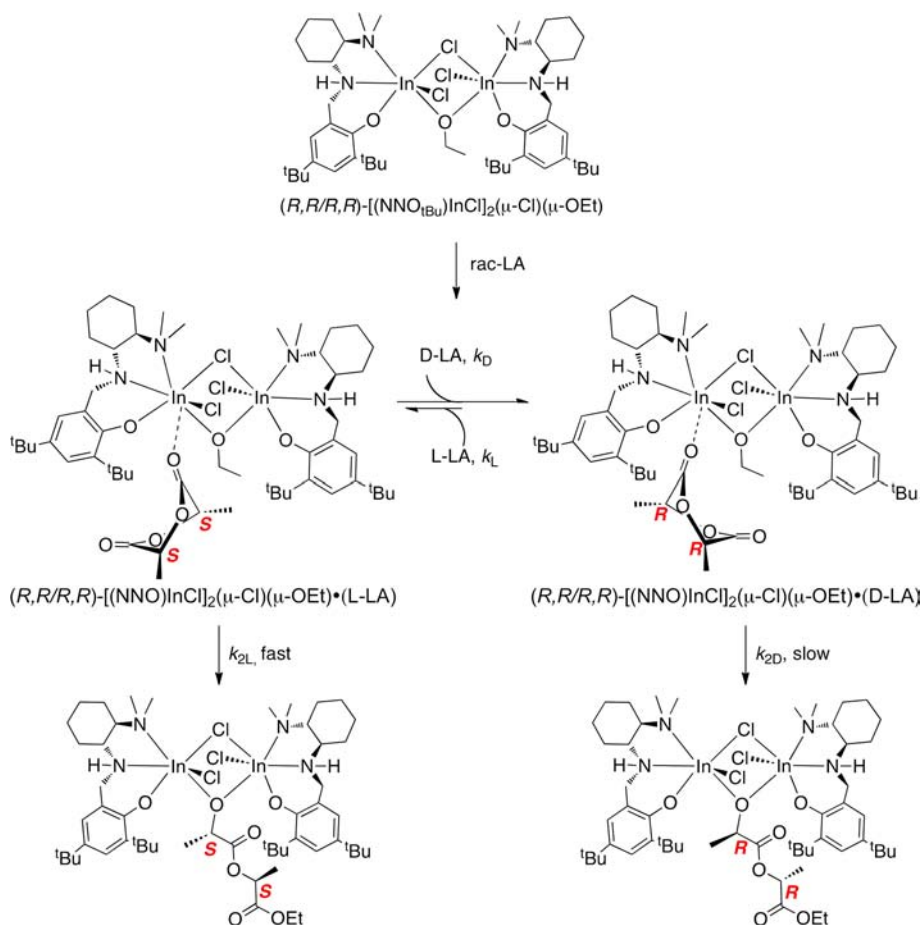


Figure 9. Plots of k_{obs} (◆) observed PLA M_n (■) as functions of added **1** for polymerization of LA with catalysts **5** ($[\text{S}] = 0.0024 \text{ M}$, CD_2Cl_2 , room temperature; M_n = number averaged molecular weight).

this dissociation does not play a role in the polymerization of lactide.

DISCUSSION AND CONCLUSIONS

We have synthesized a family of dinuclear ethoxy-bridged indium complexes $[(\text{NNO}_R)\text{InX}]_2(\mu\text{-OEt})(\mu\text{-Y})$ ($R = t\text{-Bu}$, Me; $X = \text{Cl}$, I; $Y = \text{Cl}$, I, OH, OEt) and their enantiopure analogues, and compared the reactivity of mono- ($Y = \text{Cl}$, I) and bis-alkoxy-bridged ($Y = \text{OEt}$) complexes for the living ring-opening polymerization (ROP) of lactide (LA). In particular, the chloro-ethoxy-bridged derivative $[(\text{NNO}_{t\text{Bu}})\text{InCl}]_2(\mu\text{-OEt})(\mu\text{-Cl})$ (**5**) is one of the most successful catalysts for controlled LA ROP and generates PLA samples of greater than 350 kDa with predictable molecular weights and low molecular weight distributions. The living nature of the propagation was confirmed by in situ monitoring of reactions as well as by analysis of bulk polymer samples. Kinetics studies show that after an induction period, the rate of lactide polymerization is first order in the concentration of lactide and also first order in the concentration of catalyst. Importantly, the second-order

Scheme 6. Dissociation of Bulkier Dinuclear Catalysts with Added Lactide^{19b}Scheme 7. Competing Coordination and Ring-Opening in the Reactivity of $(R,R/R,R)$ -5 with *rac*-LA

rate constants are the same regardless of whether one or two bridging ethoxy groups are present.

Complex **5** is a unique asymmetrically bridged dinuclear catalyst with excellent potential as a commercial catalyst for the ring-opening polymerization (ROP) of lactide (LA).³⁸ The dinuclear nature of the catalyst raises an important mechanistic question: Is the propagating species derived from the dissociation of the dimer in the presence of a large concentration of lactide, or does the dinuclear complex itself act as the propagating species? The data presented above support a dinuclear propagating species.

The Ethoxy-Bridged Indium Complexes Are Dinuclear in Solution. Indium alkoxide complexes in this family are invariably dinuclear in the solid state. A variety of techniques (VT NMR spectroscopy, 2D NOESY spectroscopy, PGSE experiments) confirm that the complexes are also dinuclear in solution and that the solution structures correlate closely to the solid state structures. This is most striking when comparing the

enantiopure analogues of the bis-ethoxy-bridged complex. The solid-state structure of $[(\pm)\text{-H}(\text{NNO}_R)\text{In}(\text{I})(\text{OEt})]_2$ derived from $(\pm)\text{-H}(\text{NNO}_R)$ (Figure 1) is in the centrosymmetric *meso* form, while the enantiopure $(S,S/S,S)$ -**8** has lost the center of symmetry (Figure 4). These differences are reflected in the solution structures of the compounds: $(R,R/R,R)$ - and $(S,S/S,S)$ -**8** have a ¹H NMR signature different from that of *meso*-**8** (Figure 3).

There is ample evidence that the dinuclear complexes dissociate in solution and can react with added donors under forcing conditions; however, the dinuclear complexes are the thermodynamic sinks in these systems. All irreversible reactions with added donors/complexes (Scheme 5) as well as conversion of enantiopure to *meso* complexes (Figure S21) result in the formation of more stable dinuclear complexes. The most telling experiment is the low reactivity of complex **5** with neat pyridine at 100 °C. Thus, addition of a large concentration

of a donor such as lactide does not necessarily lead to dissociation of the dimer.

Polymerization Rate and Polymer Molecular Weight Are Not Affected by Addition of $(\text{NNO}_{\text{tBu}})\text{InCl}_2$. Although an equilibrium between **5**, **1**, and a mononuclear ethoxy complex $(\text{NNO}_{\text{tBu}})\text{In}(\text{OEt})(\text{Cl})$ is possible, it does not affect the rate of polymerization nor the molecular weights of the resulting polymers (Figure 9). If complex **5** was a dormant species requiring dissociation to complex **1** and an active $(\text{NNO}_{\text{tBu}})\text{In}(\text{OEt})(\text{Cl})$, then addition of **1** would be expected to shift the equilibrium toward complex **5** and, in turn, lower rates of polymerization and lead to higher observed molecular weights. The lack of influence of added **1** on the reaction rates and polymer properties confirms that an equilibrium between the dinuclear complex **5** and the monometallic compounds **1** and $(\text{NNO}_{\text{tBu}})\text{In}(\text{OEt})(\text{Cl})$, if it is indeed present, is not important to propagation, and thus complex **5** is not a dormant species, but rather a dinuclear active catalyst as shown in Scheme 2B.

There Is No Evidence for Dissociation of **5 during Polymerization.** The mechanism in Scheme 2A assumes that the induction period is caused by the dissociation of $[(\text{NNO}_{\text{tBu}})\text{InCl}_2](\mu\text{-Cl})(\mu\text{-OEt})$ (**5**) to give lactide adducts of $(\text{NNO}_{\text{tBu}})\text{In}(\text{OEt})(\text{Cl})$, the proposed active catalyst, and $(\text{NNO}_{\text{tBu}})\text{InCl}_2$ (**1**) in the presence of lactide. We have never observed complex **1** in solution during polymerization (Figure S50); however, we have observed such dissociation in bulkier systems. In a related work with bulky N-alkylated ligands, the dinuclear catalyst $[(\text{N}_{\text{nPr}}\text{NO})\text{InCl}_2](\mu\text{-Cl})(\mu\text{-OEt})$ dissociates in the presence of added lactide to form $[(\text{N}_{\text{nPr}}\text{NO}_{\text{tBu}})\text{In}(\text{Cl})\text{(O-polymer)}]$ and $(\text{N}_{\text{nPr}}\text{NO}_{\text{tBu}})\text{InCl}_2$ (Scheme 6).^{19b} Interestingly, in the bulkier systems that dissociate, all stereoselectivity for polymerization of *rac*-LA is lost, suggesting that the selectivity observed for complex **5** is a result of its dinuclear nature.

The Mono- and Bis-Alkoxy-Bridged Complexes Show Different Selectivities for the ROP of Lactide. One of the most striking pieces of evidence for the dinuclear nature of the propagating species is the difference of selectivities observed for the mono- and bis-ethoxy bridged complexes **5** and **8**. If the propagating species is a mononuclear alkoxide, then complexes **5** and **8** should have identical selectivities. A comparison of polymerization rates with $(R,R/R,R)$ -**5** (Table 3, entry 5) and $(R,R/R,R)$ -**8** (Table 4, entry 5) shows P_m values of 0.48 and 0.65, respectively. Indeed, the different k_{rel} values for **5** and **8** (14 vs 2), and the general independence of selectivity on catalyst chirality for complex **8**, indicate that the two catalysts cannot have identical propagating species. The different solution structures of the dinuclear complexes, matched by the solid-state structures, are a strong justification for their different selectivities. The nonlinear nature of the dependence of the observed rate constant on enantiopurity of **5** (Figure 7a) also supports a dinuclear propagating species.

These observations lead us to propose an alternate mechanism for the ring-opening polymerization of lactide by our dinuclear catalysts. It is clear that ethoxy-bridged indium complexes of the type $[(\text{NNO}_R)\text{InX}]_2(\mu\text{-OEt})(\mu\text{-Y})$ ($X = \text{Cl}, \text{I}$; $Y = \text{Cl}, \text{I}, \text{OH}, \text{OEt}$) remain dinuclear during the ROP of LA. However, our studies show that the mechanism depicted in Scheme 2B is too simplistic to explain the selectivities observed for this system. In particular, there is a high k_{rel} value for polymerization of L-LA as compared to D-LA with $(R,R/R,R)$ -**5**;

however, the polymer obtained in the polymerization or *rac*-LA with this catalyst is atactic.

An alternate mechanism that better explains this phenomenon involves two competing rates: the rate of coordination of L- and D-LA to the catalyst (k_L and k_D) and the rates of propagation of these monomers (k_{2L} and k_{2D}) (Scheme 7). We know that k_{2L}/k_{2D} is 14 for $(R,R/R,R)$ -**5**. However, these values were determined using enantiopure catalyst and enantiopure monomer. When racemic lactide is added, there will be a competition between coordination of D- or L-LA to $(R,R/R,R)$ -**5**. We propose that $k_D > k_L$ and that the equilibrium favors the formation of the adduct $(R,R/R,R)$ -**5**-D-LA, which goes on to ring open D-LA. If the rates k_D and k_{2L} are on the same order, we would expect an equal incorporation of L- and D-LA into the polymer to form atactic PLA. This mechanism is compatible with the nonlinear decrease in the polymerization rate for *rac*-LA with increasing enantiopurity of catalyst (Figure 8a). We are assuming that for ROP of *rac*-LA with $(R,R/R,R)$ -**5**, chain end control is surpassed by the high selectivity of the catalyst. With (\pm) -**5** and with all isomers of **8**, chain end control dominates to yield similar P_m values (~ 0.6).

In conclusion, we studied the polymerization behavior and selectivity of chiral alkoxy-bridged dinuclear indium complexes for the ring-opening polymerization of lactide. We were able to show that the complexes remain dinuclear during lactide polymerization, with a stable dinuclear polymeryl-bridged steady state that resists chain termination and leads to a highly controlled system. The dinuclear nature of the chiral catalyst has a significant effect on the stereoselectivity of the catalysts and will impact the design of future indium-based catalysts.

EXPERIMENTAL SECTION

General Considerations. Unless otherwise indicated, all air- and/or water-sensitive reactions were carried out under dry nitrogen using either an MBraun glovebox or standard Schlenk line techniques. NMR spectra were recorded on a Bruker Avance 400 and 600 MHz spectrometer. ¹H NMR chemical shifts are reported in ppm versus residual protons in deuterated solvents as follows: δ 7.27 CDCl₃, δ 5.32 CD₂Cl₂. ¹³C{¹H} NMR chemical shifts are reported in ppm versus residual ¹³C in the solvent: δ 77.2 CDCl₃, δ 54.0 CD₂Cl₂. Diffraction measurements for X-ray crystallography were made on a Bruker X8 APEX II diffraction with graphite monochromated Mo K α radiation. The structures (Table S3) were solved by direct methods and refined by full-matrix least-squares using the SHELXTL crystallographic software of Bruker-AXS. Unless specified, all non-hydrogen were refined with anisotropic displacement parameters, and all hydrogen atoms were constrained to geometrically calculated positions but were not refined. EA CHN analysis was performed using a Carlo Erba EA1108 elemental analyzer. The elemental composition of unknown samples was determined by using a calibration factor. The calibration factor was determined by analyzing a suitable certified organic standard (OAS) of a known elemental composition. Molecular weights were determined by triple detection gel permeation chromatography (GPC-LLS) using a Waters liquid chromatograph equipped with a Water 515 HPLC pump, Waters 717 plus autosampler, Waters Styragel columns (4.6 \times 300 mm) HR5E, HR4 and HR2, Water 2410 differential refractometer, Wyatt tristar miniDAWN (laser light scattering detector), and a Wyatt ViscoStar viscometer. A flow rate of 0.5 mL min⁻¹ was used, and samples were dissolved in tetrahydrofuran (THF) (2 mg mL⁻¹). Narrow molecular weight polystyrene standards were used for calibration purposes.

Materials. Solvents (THF, toluene, hexane, and diethyl ether) were collected from an MBraun Solvent Purification System whose columns are packed with activated alumina. CH₂Cl₂ and CHCl₃ were dried over CaH₂ and degassed through a series of freeze–pump–thaw cycles. CD₂Cl₂, CDCl₃, methanol, ethanol, isopropanol, ethyl acetate,

pyridine, and acetonitrile (CH_3CN) were dried over CaH_2 , collected by vacuum distillation, and degassed through a series of freeze–pump–thaw cycles. *rac*-LA ($[\alpha]_{\text{D}} = -0.1^\circ$, toluene, 25°C), *D*-LA ($[\alpha]_{\text{D}} = +287$ to $+300^\circ$, toluene, 25°C), and *L*-LA ($[\alpha]_{\text{D}} = -288.1^\circ$, toluene, 25°C) were gifts from PURAC America Inc. and were recrystallized twice from hot dried toluene prior to use. (1*R*,2*R*)- or (1*S*,2*S*)-1,2-diaminocyclohexane was resolved from (\pm)-*trans*-1,2-diaminocyclohexane followed by the literature procedures.³⁹ KOEt was generated by reacting KO^tBu with dried ethanol. The solvent was removed under high vacuum, and addition of hexane to the residual precipitates a white solid. The white solid, KOEt, was isolated by vacuum filtration and dried in vacuo for 4 h. 1,3,5-Trimethoxybenzene and tetrakis(trimethylsilyl)silane (TMSS) were purchased from Aldrich and Alfa Aesar, respectively, and used as received. *para*-Methyl salicaldimine (see the Supporting Information), proligand $\text{H}(\text{NNO}_{t\text{Bu}})$, and complexes **1**, **2**, and **5** were synthesized according to previously reported procedures.^{17,31}

Synthesis of 6-*tert*-Butyl-2-{*N*-[2-(*N,N*-dimethyl)aminocyclohexyl]salicaldimino}-4-methylphenol (\pm)-*H*(NNO_{Me}), (*R,R*)-, and (*S,S*)-*H*(NNO_{Me}). A 500 mL round-bottom flask was charged with *para*-methyl salicaldimine (2.87 g, 9.08 mmol) (see the Supporting Information) in 150 mL of acetonitrile. NaBH_4 (2.51 g, 66.3 mmol) was added to the stirring mixture. The reaction mixture was stirred for 30 min, and a 1.5 mL solution of glacial acetic acid was added dropwise to the stirring mixture. The reaction mixture was stirred for 16 h. After the basic aqueous workup with 1 M NaOH and 5% MeOH/ CH_2Cl_2 , the organic layer was collected, and the off-white solid was obtained by removal of the solvent under vacuum. The solid was recrystallized from acetonitrile (2.17 g, 78%). ^1H NMR (600 MHz, CDCl_3): δ 7.01 (1H, br s, ArH), 6.74 (1H, br s, ArH), 4.01 (d, 1H, $^4J_{\text{H-H}} = 13.4$ Hz, NH- CH_2 -Ar), 3.81 (1H, d, $^4J_{\text{H-H}} = 13.4$ Hz, NH- CH_2 -Ar), 3.38 (1H, br s, -NH-), 2.36–2.43 (1H, m, -CH- of DACH), 2.25–2.33 (4H, m, Ar- CH_3 ; -CH- of DACH), 2.23 (6H, s, -N(CH_3)₂), 2.14–2.20 (1H, m, - CH_2 - of DACH), 1.80–1.89 (2H, m, - CH_2 - of DACH), 1.68–1.75 (1H, m, - CH_2 - of DACH), 1.45 (9H, br s, Ar-(CH_3)₃), 1.11–1.29 (4H, m, - CH_2 - of DACH). $^{13}\text{C}\{^1\text{H}\}$ NMR (151 MHz, CDCl_3): δ 154.8 (Ar C), 136.4 (Ar C), 126.6 (Ar C-H), 126.5 (Ar C-H), 126.1 (Ar C), 124.3 (Ar C), 66.6 (CH-N(CH_3)₂), 58.9 (CH-NH- CH_2), 51.1 (N-CH- CH_2), 40.0 (N(CH_3)₂), 34.5 (N(CH_3)₂), 34.5 (Ar-C(CH_3)₃), 31.7 (Ar- CH_3), 29.6 (Ar-C(CH_3)₃), 25.3 (- CH_2 - of DACH), 20.9 (- CH_2 - of DACH), 20.8 (- CH_2 - of DACH). (\pm)-*H*(NNO_{Me}). Anal. Calcd for $\text{C}_{20}\text{H}_{34}\text{N}_2\text{O}$: C, 75.42; H, 10.76; N, 8.80. Found: C, 75.36; H, 10.72; N, 8.87. (*R,R*)-*H*(NNO_{Me}), yield (0.75 g, 52%) based on 1.44 g of (*R,R*)-*para-tert*-butyl salicaldimine. Anal. Calcd for $\text{C}_{20}\text{H}_{34}\text{N}_2\text{O}$: C, 75.42; H, 10.76; N, 8.80. Found: C, 75.25; H, 10.76; N, 8.69. (*S,S*)-*H*(NNO_{Me}), yield (0.42 g, 50%) based on 0.83 g of (*S,S*)-*para*-methyl salicaldimine. Anal. Calcd for $\text{C}_{20}\text{H}_{34}\text{N}_2\text{O}$: C, 75.42; H, 10.76; N, 8.80. Found: C, 75.07; H, 10.62; N, 8.45.

Synthesis of 4,6-Di-*tert*-butyl-2-{*N*-[2-(*N,N*-dimethyl)aminocyclohexyl]salicaldimino}phenol (*R,R*)- and (*S,S*)-*H*($\text{NNO}_{t\text{Bu}}$). The syntheses were carried out in a manner analogous to that of the racemic compound above and have identical NMR signatures.¹⁷ (*R,R*)-*H*($\text{NNO}_{t\text{Bu}}$), yield (1.88 g, 59%) based on 3.14 g of (*R,R*)-*para-tert*-butyl salicaldimine. Anal. Calcd for $\text{C}_{23}\text{H}_{40}\text{N}_2\text{O}$: C, 76.61; H, 11.18; N, 7.77. Found: C, 76.44; H, 11.29; N, 7.65. (*S,S*)-*H*($\text{NNO}_{t\text{Bu}}$), yield (0.35 g, 50%) based on 0.70 g of (*S,S*)-*para-tert*-butyl salicaldimine. Anal. Calcd for $\text{C}_{23}\text{H}_{40}\text{N}_2\text{O}$: C, 76.61; H, 11.18; N, 7.77. Found: C, 75.10; H, 11.23; N, 7.84.

Synthesis of (*R,R*)- and (*S,S*)-($\text{NNO}_{t\text{Bu}}$) InCl_2 (1**).** The syntheses of (\pm)- and (*R,R*)- $\text{NNO}_{t\text{Bu}}\text{InCl}_2$ were published previously in the literature.¹⁷ (*S,S*)-($\text{NNO}_{t\text{Bu}}$) InCl_2 was carried out in a manner analogous to that of (\pm)- and (*R,R*)-(**1**), and they have identical NMR signatures. A 20 mL scintillation was charged with $\text{H}(\text{NNO}_{\text{Me}})$ (198 mg, 0.62 mmol) in toluene (5 mL) at room temperature. Benzyl potassium (76.8 mg, 0.59 mmol) in toluene (5 mL) as a slurry was added dropwise to the stirring solution at room temperature. The reaction mixture was stirred for 16 h. An off-white solid was isolated by removal of the solvent under high vacuum. The product, $\text{K}(\text{NNO}_{t\text{Bu}})$, was used for further reaction without any other purification and

characterization. A suspension of InCl_3 (81.6 mg, 0.37 mmol) in THF (3 mL) was added dropwise to a slurry of $\text{K}(\text{NNO}_{\text{Me}})$ (147 mg, 0.37 mmol) in THF (10 mL). The mixture was stirred for 16 h at room temperature resulting in a white solid (KCl) and yellow solution. The white solid was filtered through Celite, and the pale yellow filtrate was concentrated under vacuum. The residue was taken up in 3 mL of Et_2O , from which an off-white solid precipitated. The solid was isolated by vacuum filtration and dried in vacuo for a few hours. (*S,S*)-($\text{NNO}_{t\text{Bu}}$) InCl_2 , yield (153 mg, 76%). ^1H NMR (600 MHz, CD_2Cl_2): δ 7.28 (1H, br s, ArH), 6.89 (1H, br s, ArH), 4.14 (2H, br s, NH- CH_2 -Ar), 2.73 (3H, s, N-(CH_3)₂), 2.54–2.69 (3H, m, -NH- and -CH- of DACH), 2.44 (3H, br s, -N-(CH_3)₂), 2.01–2.13 (2H, m, - CH_2 - of DACH), 1.82–1.98 (2H, m, - CH_2 - of DACH), 1.42 (9H, br s, Ar-(CH_3)₃), 1.16–1.36 (13H, m, - CH_2 - of DACH and Ar-(CH_3)₃). $^{13}\text{C}\{^1\text{H}\}$ NMR (151 MHz, CD_2Cl_2): δ 164.1 (Ar C), 140.2 (Ar C), 130.4 (Ar C-H), 125.3 (Ar C-H), 125.3 (Ar C), 121.9 (Ar C), 66.7 (N-CH- CH_2), 56.0 (N-CH- CH_2), 52.4 (N- CH_2 -Ar), 44.6 (N(CH_3)₂), 38.1 (N(CH_3)₂), 35.6 (Ar-C(CH_3)₃), 34.5 (Ar-C(CH_3)₃), (32.0 (Ar-C(CH_3)₃), 31.9 (- CH_2 - of DACH), 30.2 (Ar-C(CH_3)₃), 25.0 (2C, - CH_2 - of DACH), 22.5 (- CH_2 - of DACH). (*S,S*)-($\text{NNO}_{t\text{Bu}}$) InCl_2 , Anal. Calcd for $\text{C}_{23}\text{H}_{39}\text{Cl}_2\text{InN}_2\text{O}$: C, 50.66; H, 7.21; N, 5.14. Found: C, 50.57; H, 7.06; N, 5.14. (*R,R*)-($\text{NNO}_{t\text{Bu}}$) InCl_2 , yield (231 mg, 80%) based on 211 mg of (*R,R*)- $\text{K}(\text{NNO}_{t\text{Bu}})$. Anal. Calcd for $\text{C}_{23}\text{H}_{39}\text{Cl}_2\text{InN}_2\text{O}$: C, 50.66; H, 7.21; N, 5.14. Found: C, 50.39; H, 7.20; N, 5.39.

Synthesis of (NNO_{Me}) InCl_2 (3**).** A 100 mL round-bottom flask was charged with $\text{H}(\text{NNO}_{\text{Me}})$ (309 mg, 0.97 mmol) in toluene (30 mL) at room temperature. Benzyl potassium (126 mg, 0.97 mmol) in toluene (30 mL) was added dropwise to the stirring solution at room temperature. The reaction mixture was stirred for 16 h. An off-white solid was isolated by removal of the solvent under high vacuum. The product, $\text{K}(\text{NNO}_{\text{Me}})$, was used further in the reaction without any other purification and characterization. A suspension of InCl_3 (239 mg, 1.08 mmol) in THF (3 mL) was added dropwise to a slurry of $\text{K}(\text{NNO}_{\text{Me}})$ in THF (10 mL). The mixture was stirred for 16 h at room temperature, resulting in a white solid (KCl) and yellow solution. The white solid was filtered through Celite, and the pale yellow filtrate was concentrated under vacuum. The residue was taken up in 5 mL of Et_2O , from which an off-white solid precipitated. The solid was isolated by vacuum filtration and dried in vacuo for a few hours. Recrystallization with a mixture solution of THF and ether at room temperature afforded yellow crystals of **3** (380 mg, 76%). ^1H NMR (400 MHz, CD_2Cl_2): δ 7.04 (1H, d, $^4J_{\text{H-H}} = 2.0$ Hz, ArH), 6.68 (1H, d, $^4J_{\text{H-H}} = 1.7$ Hz, ArH), 4.46 (1H, d, $^2J_{\text{H-H}} = 12.6$ Hz, NH- CH_2 -Ar), 3.97 (1H, dd, $^2J_{\text{H-H}} = 12.5$ Hz, $^3J_{\text{H-H}} = 6.7$ Hz, NH- CH_2 -Ar), 2.73–2.82 (1H, m, -CH- of DACH), 2.71 (3H, s, -N-(CH_3)₂), 2.63–2.61 (1H, m, -CH- of DACH), 2.54 (1H, br s, -NH- of DACH), 2.38–2.48 (1H, m, - CH_2 - of DACH), 2.27 (3H, s, -N-(CH_3)₂), 2.21 (3H, s, Ar- CH_3), 1.94–2.04 (m, 1H, - CH_2 - of DACH), 1.78–1.94 (2H, m, - CH_2 - of DACH), 1.40 (9H, Ar-(CH_3)₃), 1.18–1.29 (4H, m, - CH_2 - of DACH). $^{13}\text{C}\{^1\text{H}\}$ NMR (151 MHz, CD_2Cl_2): δ 161.9 (Ar C), 140.2 (Ar C), 129.7 (Ar C-H), 125.0 (Ar C-H), 128.9 (Ar C), 121.4 (Ar C), 66.2 (N- CH_2 -Ar), 54.8 (N-CH- CH_2), 51.0 (N-CH- CH_2), 44.7 (N(CH_3)₂), 38.4 (N(CH_3)₂), 35.3 (Ar-C(CH_3)₃), 31.5 (Ar- CH_3), 30.3 (Ar-C(CH_3)₃), 25.0 (- CH_2 - of DACH), 22.4 (- CH_2 - of DACH), 20.9 (- CH_2 - of DACH). Anal. Calcd for $\text{C}_{20}\text{H}_{33}\text{Cl}_2\text{InN}_2\text{O}$: C, 47.74; H, 6.61; N, 5.57. Found: C, 47.48; H, 6.60; N, 5.51.

Synthesis of (\pm)-, (*R,R*)-, and (*S,S*)-(NNO_{Me}) InI_2 (4**).** Complex **4** was synthesized in a manner similar to that of **3** by adding a suspension of InI_3 (973 mg, 1.96 mmol) in THF (3 mL) to a slurry of $\text{K}(\text{NNO}_{\text{Me}})$ (700 mg, 1.96 mmol) in THF (20 mL). Complex **4** was obtained on a glass frit and dried in vacuo for a few hours (965 mg, 72%). ^1H NMR (600 MHz, CD_2Cl_2): δ 7.04 (1H, d, $^4J_{\text{H-H}} = 1.8$ Hz, ArH), 6.70 (1H, d, $^4J_{\text{H-H}} = 1.5$ Hz, ArH), 4.05–4.11 (1H, m, NH- CH_2 -Ar), 3.94 (1H, d, $^2J_{\text{H-H}} = 11.1$ Hz, NH- CH_2 -Ar), 2.72–2.78 (1H, m, -CH- of DACH), 2.63–2.69 (1H, m, -CH- of DACH), 2.61 (3H, s, -N-(CH_3)₂), 2.54–2.58 (1H, m, - CH_2 - of DACH), 2.45 (3H, s, -N-(CH_3)₂), 2.21 (3H, s, Ar- CH_3), 2.06–2.11 (1H, m, - CH_2 - of DACH), 1.81–1.96 (2H, m, -NH-; - CH_2 - of DACH),

1.76 (1H, m, $-\text{CH}_2-$ of DACH), 1.42 (9H, Ar- $(\text{CH}_3)_3$), 1.17–1.40 (4H, m, $-\text{CH}_2-$ of DACH). $^{13}\text{C}\{^1\text{H}\}$ NMR (151 MHz, CD_2Cl_2): δ 161.3 (Ar C), 140.9 (Ar C), 129.0 (Ar C–H), 128.6 (Ar C–H), 125.6 (Ar C), 122.7 (Ar C), 65.5 (N– CH_2 –Ar), 56.7 (N–CH– CH_2), 52.4 (N–CH– CH_2), 43.9 (N(CH_3) $_2$), 37.7 (N(CH_3) $_2$), 35.1 (Ar–C(CH_3) $_3$), 32.4 (Ar– CH_3), 30.6 (Ar–C(CH_3) $_3$), 25.1 ($-\text{CH}_2-$ of DACH), 25.0 ($-\text{CH}_2-$ of DACH), 23.1 ($-\text{CH}_2-$ of DACH), 21.0 ($-\text{CH}_2-$ of DACH). (\pm)-(NNO_{Me})InI₂. Anal. Calcd for $\text{C}_{20}\text{H}_{33}\text{I}_2\text{InN}_2\text{O}$: C, 35.01; H, 4.85; N, 4.08. Found: C, 35.11; H, 4.79; N, 4.08. (R,R)-(NNO_{Me})InI₂. The syntheses were carried out in a manner analogous to that of the racemic compound above and have identical NMR signatures. Yield (286 mg, 85%) based on 173 mg of (R,R)-K(NNO_{Me}). Anal. Calcd for $\text{C}_{20}\text{H}_{33}\text{I}_2\text{InN}_2\text{O}$: C, 35.01; H, 4.85; N, 4.08. Found: C, 34.90; H, 4.85; N, 4.03. (S,S)-(NNO_{Me})InI₂. The syntheses were carried out in a manner analogous to that of the racemic compound above and have identical NMR signatures. Yield (162 mg, 80%) based on 105 mg of (S,S)-K(NNO_{Me}). Anal. Calcd for $\text{C}_{20}\text{H}_{33}\text{I}_2\text{InN}_2\text{O}$: C, 35.01; H, 4.85; N, 4.08. Found: C, 34.90; H, 4.85; N, 4.03. (S,S)-(NNO_{Me})InI₂. The syntheses were carried out in a manner analogous to that of the racemic compound above and have identical NMR signatures. Yield (162 mg, 80%) based on 105 mg of (S,S)-K(NNO_{Me}). Anal. Calcd for $\text{C}_{20}\text{H}_{33}\text{I}_2\text{InN}_2\text{O}$: C, 35.01; H, 4.85; N, 4.08. Found: C, 34.90; H, 4.85; N, 4.03.

Synthesis of (R,R/R,R)- and (S,S/S,S)-[(NNO_{tBu})InCl₂(μ -Cl)(μ -OEt) (5). The syntheses were carried out in a manner analogous to that of the racemic compound and have identical NMR signatures.¹⁷ (R,R/R,R)-5, yield (28 mg, 87%) based on 32 mg of (R,R)-(NNO_{tBu})InCl₂. Anal. Calcd for $\text{C}_{48}\text{H}_{84}\text{Cl}_3\text{In}_2\text{N}_4\text{O}_3$: C, 52.40; H, 7.60; N, 5.09. Found: C, 51.97; H, 7.54; N, 4.95. (S,S/S,S)-5, yield (53 mg, 85%) based on 61 mg of (S,S)-(NNO_{tBu})InCl₂. Anal. Calcd for $\text{C}_{48}\text{H}_{84}\text{Cl}_3\text{In}_2\text{N}_4\text{O}_3$: C, 52.40; H, 7.60; N, 5.09. Found: C, 52.16; H, 7.51; N, 5.34.

Synthesis of [(NNO_{Me})InCl₂(μ -Cl)(μ -OEt) (6). A solution of NaOEt (20 mg, 0.30 mmol) in toluene (1.5 mL) was added dropwise to a stirring suspension of complex 3 (150 mg, 0.30 mmol) in toluene (3 mL) at room temperature. The reaction mixture was stirred for 12 h. The resulting white precipitate was filtered through Celite to yield a pale yellow filtrate. All volatiles were removed in vacuo, and ether (5 mL) was added to the residue to precipitate an off-white solid. The product was collected on a glass frit by vacuum filtration, washed with ether at least twice, and dried in vacuo for a few hours (140.8 mg, 93%). ^1H NMR (400 MHz, CD_2Cl_2): δ 6.99 (1H, br s, ArH), 6.60 (1H, br s, ArH), 4.91 (1H, d, $^2J_{\text{H-H}} = 13.5$ Hz, NH– CH_2 –Ar), 4.25–4.45 (1H, m, O– CH_2 – CH_3), 3.72 (1H, dd, $^2J_{\text{H-H}} = 13.6$ Hz, $^3J_{\text{H-H}} = 1.7$ Hz, NH– CH_2 –Ar), 2.86 (1H, td, $^3J_{\text{H-H}} = 11.3$, $^4J_{\text{H-H}} = 3.1$ Hz, $-\text{CH}-$ of DACH), 2.73–2.74 (1H, br m, $-\text{NH}-$), 2.66 (3H, s, $-\text{N}(\text{CH}_3)_2$), 2.52–2.63 (1H, m, $-\text{CH}-$ of DACH), 2.48–2.50 (1H, m, $-\text{CH}_2-$ of DACH), 2.18 (3H, s, Ar– CH_3), 2.03 (3H, s, $-\text{N}(\text{CH}_3)_2$), 1.86–1.99 (1H, m, $-\text{CH}_2-$ of DACH), 1.82 (2H, br m, $-\text{CH}_2-$ of DACH), 1.39 (9H, Ar– $(\text{CH}_3)_3$), 1.01–1.31 (6H, m, $-\text{CH}_2-$ of DACH; O– CH_2 – CH_3). $^{13}\text{C}\{^1\text{H}\}$ NMR (101 MHz, CD_2Cl_2): δ 163.2 (Ar C), 139.9 (Ar C), 130.6 (Ar C–H), 128.6 (Ar C–H), 123.3 (Ar C), 120.0 (Ar C), 65.3 (N– CH_2 –Ar), 63.0 (O– CH_2 – CH_3), 53.2 (N–CH– CH_2), 50.8 (N–CH– CH_2), 44.6 (N– $(\text{CH}_3)_2$), 38.5 (N(CH_3) $_2$), 35.5 (Ar–C(CH_3) $_3$), 31.5 (Ar– CH_3), 30.2 (Ar–C(CH_3) $_3$), 25.4 ($-\text{CH}_2-$ of DACH), 25.2 ($-\text{CH}_2-$ of DACH), 22.4 ($-\text{CH}_2-$ of DACH), 20.9 ($-\text{CH}_2-$ of DACH), 19.8 (O– CH_2 – CH_3). Anal. Calcd for $\text{C}_{42}\text{H}_{71}\text{Cl}_3\text{In}_2\text{N}_4\text{O}_3$: C, 49.65; H, 7.04; N, 5.51. Found: C, 48.91; H, 6.89; N, 5.29.

Synthesis of [(NNO_{Me})InI₂(μ -I)(μ -OEt) (7). NaOEt (61.3 mg, 0.90 mmol) suspended in toluene (6 mL) was added dropwise to a stirring suspension of complex 4 (309.4 mg, 0.45 mmol) in toluene (8 mL) (both of the suspensions were stirred for 5 min separately). The reaction mixture was stirred for 16 h. The resulting white precipitate was filtered through glass filter paper to collect the pale yellow filtrate. All volatiles were removed from the filtrate in vacuo, and the residue was completely dissolved in THF (2 mL). Acetonitrile (5 mL) was added to this solution after which complex 8 was isolated as a white solid via filtration. The solvent was removed from the filtrate to yield complex 7 as an off-white solid. Both complexes were washed with acetonitrile (2 \times 1 mL) and dried in vacuo for several hours (complex 7, 100.5 mg, 35% yield; complex 8, 39.5 mg, 14% yield). ^1H NMR (400 MHz, CD_2Cl_2): δ 7.00 (1H, d, $^4J_{\text{H-H}} = 1.9$ Hz, ArH), 6.63 (1H, d, $^4J_{\text{H-H}} = 1.9$ Hz, ArH), 4.79–4.86 (1H, m, NH– CH_2 –Ar), 4.15–

4.41 (1H, m, O– CH_2 – CH_3), 3.65–3.77 (1H, m, NH– CH_2 –Ar), 3.41 (1H, d, $^3J_{\text{H-H}} = 10.8$ Hz, $-\text{NH}-$), 2.60–2.72 (1H, m, $-\text{CH}-$ of DACH), 2.57 (3H, s, $-\text{N}(\text{CH}_3)_2$), 2.51–2.55 (1H, m, $-\text{CH}_2-$ of DACH), 2.46 (1H, td, $^3J_{\text{H-H}} = 11.4$ Hz, $^4J_{\text{H-H}} = 3.2$ Hz, $-\text{CH}-$ of DACH), 2.20 (3H, s, $-\text{Ar}-\text{CH}_3$), 1.96 (3H, s, $-\text{N}(\text{CH}_3)_2$), 1.84 (2H, t, $^3J_{\text{H-H}} = 12.1$ Hz, $-\text{CH}_2-$ of DACH), 1.43 (9H, Ar– $(\text{CH}_3)_3$), 1.37 (2H, t, $^3J_{\text{H-H}} = 12.1$ Hz, O– CH_2 – CH_3), 1.05–1.33 (5H, m, $-\text{CH}_2-$ of DACH). $^{13}\text{C}\{^1\text{H}\}$ NMR (101 MHz, CD_2Cl_2): δ 163.4 (Ar C), 139.7 (Ar C), 130.5 (Ar C–H), 128.4 (Ar C–H), 122.9 (Ar C), 120.3 (Ar C), 67.4 (N– CH_2 –Ar), 61.9 (O– CH_2 – CH_3), 53.2 (N–CH– CH_2), 50.0 (N–CH– CH_2), 46.0 (N(CH_3) $_2$), 38.1 (N(CH_3) $_2$), 35.3 (Ar–C(CH_3) $_3$), 31.2 (Ar– CH_3), 30.4 (Ar–C(CH_3) $_3$), 25.4 ($-\text{CH}_2-$ of DACH), 25.2 ($-\text{CH}_2-$ of DACH), 22.6 ($-\text{CH}_2-$ of DACH), 20.9 ($-\text{CH}_2-$ of DACH), 19.5 (O– CH_2 – CH_3). Anal. Calcd for $\text{C}_{42}\text{H}_{71}\text{I}_3\text{In}_2\text{N}_4\text{O}_3$: C, 39.09; H, 5.55; N, 4.34. Found: C, 42.69; H, 6.22; N, 5.48.

Synthesis of (meso)-, (R,R/R,R)-, and (S,S/S,S)-[(NNO_{Me})InI(μ-OEt)]₂ (8). A suspension of KOEt (24.5 mg, 0.29 mmol) in toluene (4 mL) was added dropwise to a stirring suspension of 4 (125.4 mg, 0.14 mmol) in toluene (6 mL) at room temperature (both of the solutions were stirred for 5 min separately prior to addition). The pale yellow color of the reaction mixture changed to white in 5 min after the addition of KOEt. The white solid was filtered through a glass filter paper to collect the colorless filtrate complex 8, which was dried in vacuo to yield an off white residue. THF (1 mL) was added to the white residue, forming a suspension. Subsequently, acetonitrile (2 mL) was added to this stirring suspension to solubilize any remaining impurities. The suspension was filtered through a glass frit, and the solid was washed with acetonitrile (2 \times 1 mL) and dried under vacuum to obtain the desired complex 8 as a white solid (81.2 mg, 74% yield). ^1H NMR (400 MHz, CD_2Cl_2): δ 6.98 (1H, br s, ArH), 6.59 (1H, br s, ArH), 5.08 (1H, d, $^2J_{\text{H-H}} = 13.3$ Hz, NH– CH_2 –Ar), 4.30–4.42 (1H, m, O– CH_2 – CH_3), 3.65–3.80 (2H, m, O– CH_2 – CH_3 , NH– CH_2 –Ar), 2.60–2.75 (5H, br s, $-\text{CH}-$ of DACH; $-\text{CH}-$ of DACH; $-\text{N}(\text{CH}_3)_2$), 2.49 (1H, m, $-\text{NH}-$ of DACH), 2.18 (3H, s, Ar– CH_3), 2.06 (3H, s, $-\text{N}(\text{CH}_3)_2$), 1.97 (1H, br m, $-\text{CH}_2-$ of DACH), 1.74–1.87 (2H, m, $-\text{CH}_2-$ of DACH), 1.39 (9H, Ar– $(\text{CH}_3)_3$), 1.05–1.23 (8H, m, $-\text{CH}_2-$ of DACH and O– CH_2 – CH_3). $^{13}\text{C}\{^1\text{H}\}$ NMR (151 MHz, CD_2Cl_2): δ 163.5 (Ar C), 139.7 (Ar C), 130.4 (Ar C–H), 128.4 (Ar C–H), 122.4 (Ar C), 120.0 (Ar C), 68.3 (N–CH– CH_2), 60.8 (O– CH_2 – CH_3), 52.6 (N– CH_2 –Ar), 51.4 (N–CH– CH_2), 49.9 (N(CH_3) $_2$), 40.0 (N(CH_3) $_2$), 35.3 (Ar–C(CH_3) $_3$), 31.1 (Ar– CH_3), 30.4 (Ar–C(CH_3) $_3$), 25.4 ($-\text{CH}_2-$ of DACH), 25.1 ($-\text{CH}_2-$ of DACH), 23.3 ($-\text{CH}_2-$ of DACH), 20.9 ($-\text{CH}_2-$ of DACH), 19.7 (O– CH_2 – CH_3). (meso)-8, Anal. Calcd for $\text{C}_{44}\text{H}_{76}\text{I}_2\text{In}_2\text{N}_4\text{O}_4$: C, 43.73; H, 6.34; N, 4.64. Found: C, 44.09; H, 6.36; N, 4.84.

(R,R/R,R)- and (S,S/S,S)-8. The syntheses were carried out in a manner analogous to that of the racemic compound above. (R,R/R,R)-8, yield (48 mg, 60%) based on 90 mg of (R,R)-(NNO_{Me})InI₂. Anal. Calcd for $\text{C}_{44}\text{H}_{76}\text{I}_2\text{In}_2\text{N}_4\text{O}_4$: C, 43.73; H, 6.34; N, 4.64. Found: C, 44.11; H, 6.31; N, 4.65. (S,S/S,S)-8, yield (44 mg, 68%) based on 73 mg of (S,S)-(NNO_{Me})InI₂. Anal. Calcd for $\text{C}_{44}\text{H}_{76}\text{I}_2\text{In}_2\text{N}_4\text{O}_4$: C, 43.73; H, 6.34; N, 4.64. Found: C, 43.96; H, 6.34; N, 4.67. (R,R)- and (S,S)-8 have identical NMR spectra. ^1H NMR (600 MHz, CDCl_3): δ 7.02 (2H, m, ArH), 6.65–6.70 (1H, m, ArH), 6.53–6.61 (1H, m, ArH), 5.19 (1H, d, $^2J_{\text{H-H}} = 13.6$ Hz, NH– CH_2 –Ar), 4.63–4.72 (1H, m, NH– CH_2 –Ar), 4.33–4.49 (2H, m, O– CH_2 – CH_3), 3.82–3.96 (2H, m, O– CH_2 – CH_3), 3.70–3.82 (2H, m, NH– CH_2 –Ar), 2.95–3.09 (1H, m, $-\text{CH}-$ of DACH), 2.73–2.80 (1H, m, $-\text{CH}-$ of DACH), 2.60–2.73 (m, 4H, $-\text{NH}-$ of DACH and $-\text{N}(\text{CH}_3)_2$), 2.52 (1H, d, $^3J_{\text{H-H}} = 10.9$ Hz, $-\text{NH}-$ of DACH), 2.44 (3H, s, $-\text{N}(\text{CH}_3)_2$), 2.34 (3H, s, $-\text{N}(\text{CH}_3)_2$), 2.27 (1H, td, $^3J_{\text{H-H}} = 3.8$, 11.7 Hz, $-\text{NH}-$ of DACH), 2.19–2.25 (6H, m, Ar– CH_3), 2.10–2.19 (2H, m, $-\text{CH}_2-$ of DACH), 2.09 (3H, s, $-\text{N}(\text{CH}_3)_2$), 1.98 (1H, m, $-\text{CH}_2-$ of DACH), 1.78–1.91 (4H, m, $-\text{CH}_2-$ of DACH), 1.42 (19H, m, $-\text{CH}_2-$ of DACH, Ar–C(CH_3) $_3$), 1.30 (3H, t, $^3J_{\text{H-H}} = 6.7$ Hz, O– CH_2 – CH_3), 1.14–1.28 (6H, m, $-\text{CH}_2-$ of DACH), 1.11 (3H, t, $^3J_{\text{H-H}} = 6.6$ Hz, O– CH_2 – CH_3), 1.07 (1H, m, $-\text{CH}_2-$ of DACH), 0.93–1.00 (1H, m, $-\text{CH}_2-$ of DACH). $^{13}\text{C}\{^1\text{H}\}$ NMR (151 MHz, CD_2Cl_2): δ 164.0 (Ar

C), 163.0 (Ar C), 139.4 (Ar C), 138.7 (Ar C), 130.0 (Ar C-H), 129.6 (Ar C-H), 128.0 (Ar C-H), 127.8 (Ar C-H), 122.1 (Ar C), 121.9 (Ar C), 121.2 (Ar C), 119.4 (Ar C), 67.8 (N-CH-CH₂), 64.6 (N-CH-CH₂), 60.9 (O-CH₂-CH₃), 60.5 (O-CH₂-CH₃), 56.2 (N-CH-CH₂), 52.1 (N-CH-CH₂), 51.2 (N-CH₂-Ar), 47.4 (N-CH₂-Ar), 46.6 (-N(CH₃)₂), 45.3 (-N(CH₃)₂), 39.7 (-N(CH₃)₂), 38.5 (-N(CH₃)₂), 35.0 (Ar-C(CH₃)₃), 34.9 (-CH₂- of DACH), 30.7 (Ar-C(CH₃)₃), 30.4 (Ar-C(CH₃)₃), 30.1 (Ar-C(CH₃)₃), 28.8 (-CH₂- of DACH), 25.1 (-CH₂- of DACH), 25.1 (-CH₂- of DACH), 24.7 (-CH₂- of DACH), 24.6 (-CH₂- of DACH), 23.9 (-CH₂- of DACH), 22.7 (-CH₂- of DACH), 20.8 (Ar-CH₃), 20.7 (Ar-CH₃), 20.1 (O-CH₂-CH₃), 19.5 (O-CH₂-CH₃).

Synthesis of [(NNO_{tbu})In(I)(μ-OEt)]₂ (9). A 25 mL round-bottom flask was charged with a suspension of NaOEt (56 mg, 0.84 mmol) in 5 mL of THF. A solution of **2** (300 mg, 0.42 mmol) dissolved in 10 mL of THF was added dropwise to this mixture. After the reaction mixture was stirred for 2 h at room temperature, NaI formation was observed. The salt was removed by filtration through glass filter paper, and the remaining yellow solution was evaporated to dryness. The residue was washed with hexane and dried for 2 h in vacuo to yield complex **9** as a white powder (208 mg, 76% yield). ¹H NMR (600 MHz, CD₂Cl₂): δ 7.20 (1H, br s, ArH), 6.76 (1H, br s, ArH), 5.10 (1H, d, ²J_{H-H} = 13.4 Hz, NH-CH₂-Ar), 4.28–4.40 (1H, m, O-CH₂-CH₃), 3.69–3.82 (2H, m, O-CH₂-CH₃, NH-CH₂-Ar), 2.67–2.71 (5H, m, -CH- of DACH; -CH- of DACH; -N(CH₃)₂), 2.48–2.50 (1H, m, -NH-), 2.18 (3H, s, Ar-CH₃), 2.04 (3H, s, -N(CH₃)₂), 1.96 (1H, br m, -CH₂- of DACH), 1.76–1.90 (2H, m, -CH₂- of DACH), 1.40 (9H, Ar-(CH₃)₃), 1.26 (9H, m, Ar-(CH₃)₃), 1.13–1.23 (5H, m, -CH₂- of DACH; O-CH₂-CH₃), 1.02–1.13 (3H, -CH₂- of DACH). ¹³C{¹H} NMR (151 MHz, CD₂Cl₂): δ 162.2 (Ar C), 137.7 (Ar C), 135.0 (Ar C-H), 125.8 (Ar C-H), 123.3 (Ar C), 118.5 (Ar C), 67.1 (N-CH₂-Ar), 59.8 (O-CH₂-CH₃), 51.6 (N-CH-CH₂), 50.7 (N-CH-CH₂), 44.7 (N-(CH₃)₂), 39.0 (N(CH₃)₂), 34.6 (Ar-C(CH₃)₃), 33.2 (Ar-C(CH₃)₃), 31.1 (Ar-C(CH₃)₃), 30.0 (Ar-C(CH₃)₃), 29.5 (-CH₂- of DACH), 24.6 (-CH₂- of DACH), 24.2 (Ar-CH₂- of DACH), 22.3 (-CH₂- of DACH), 18.9 (O-CH₂-CH₃). Anal. Calcd for C₅₀H₈₆I₃In₂N₄O₄: C, 46.44; H, 6.65; N, 4.33. Found: C, 46.41; H, 6.60; N, 4.34.

Synthesis of [(NNO_{Me})In(I)]₂(μ-OH)(μ-OEt) (10). Deoxygenated H₂O (0.6 μL, 0.033 mmol) was added to a stirring suspension of complex **8** (50 mg, 0.041 mmol) in THF (3 mL) at room temperature. The reaction mixture was stirred for 16 h. The solvent was removed in vacuo to obtain a white solid, which was dried under vacuum to yield complex **10** as a white solid. To purify the compound, this solid was redissolved in THF (2 mL), and a 3 mL solution of acetonitrile was added to the solution to precipitate the unreacted starting complex. This suspension was filtered through a frit, and complex **8** was collected as a solid and reused for other reactions. The filtrate was isolated, and the solvent was removed to yield complex **10** as a white solid (19.5 mg, 50% yield). ¹H NMR (600 MHz, CD₂Cl₂): δ 6.97 (1H, d, ⁴J_{H-H} = 1.9 Hz, ArH), 6.61 (1H, d, ⁴J_{H-H} = 1.7 Hz, ArH), 4.77–4.82 (1H, m, NH-CH₂-Ar), 4.13–4.39 (1H, m, O-CH₂-CH₃), 3.69 (1H, dd, ²J_{H-H} = 13.6 Hz, ³J_{H-H} = 2.2 Hz, NH-CH₂-Ar), 3.39 (1H, d, ⁴J = 10.9 Hz, -NH-), 2.61–2.66 (1H, m, -CH- of DACH), 2.55 (3H, s, -N(CH₃)₂), 2.47–2.53 (1H, m, -CH₂- of DACH), 2.43 (1H, td, ³J_{H-H} = 11.4 Hz, ⁴J_{H-H} = 3.3 Hz, -CH- of DACH), 2.18 (3H, s, Ar-CH₃), 1.94 (3H, s, -N(CH₃)₂), 1.82 (2H, t, ³J_{H-H} = 15.9 Hz, -CH₂- of DACH), 1.41 (9H, Ar-(CH₃)₃), 1.34 (2H, t, ³J_{H-H} = 7.0 Hz, O-CH₂-CH₃), 1.01–1.33 (5H, m, -CH₂- of DACH). ¹³C{¹H} NMR (101 MHz, CD₂Cl₂): δ 163.3 (Ar C), 139.7 (Ar C), 130.5 (Ar C-H), 128.4 (Ar C-H), 122.9 (Ar C), 120.3 (Ar C), 67.3 (N-CH₂-Ar), 61.9 (O-CH₂-CH₃), 53.2 (N-CH-CH₂), 49.9 (N-CH-CH₂), 46.0 (N(CH₃)₂), 38.1 (N(CH₃)₂), 35.3 (Ar-C(CH₃)₃), 31.2 (Ar-CH₃), 30.3 (Ar-C(CH₃)₃), 25.4 (-CH₂- of DACH), 25.1 (-CH₂- of DACH), 22.6 (-CH₂- of DACH), 20.9 (-CH₂- of DACH), 19.5 (O-CH₂-CH₃). Anal. Calcd for C₄₂H₇₁I₃In₂N₄O₃: C, 42.73; H, 6.15; N, 4.75. Found: C, 43.26; H, 6.20; N, 5.40.

Synthesis of [(NNO_{tbu})In(I)]₂(μ-OH)(μ-OEt) (11). A 25 mL round-bottom flask was charged with a solution of **5** (250 mg, 0.19 mmol) in 10 mL of CH₂Cl₂, and then water (3.5 μL, 0.19 mmol) was added to

the solution. The reaction was stirred for 1 h, and after that the mixture was evaporated to dryness in vacuo. The residue was washed with diethyl ether and dried for 2 h in vacuo, to yield complex **11** as a white powder. Suitable crystals for X-ray diffraction were grown by slow diffusion on diethyl ether in a CH₂Cl₂ solution of the complex (204.1 mg, 85% yield). ¹H NMR (600 MHz, CD₂Cl₂): δ 7.20 (1H, d, ⁴J_{H-H} = 3 Hz, ArH), 6.78 (1H, d, ⁴J_{H-H} = 3 Hz, ArH), 4.81 (1H, d, ²J_{H-H} = 13.2 Hz, NH-CH₂-Ar), 4.14–4.44 (1H, m, O-CH₂-CH₃), 3.73 (1H, d, ²J_{H-H} = 13.3 Hz, NH-CH₂-Ar), 3.42 (1H, d, ³J_{H-H} = 10.8 Hz, -NH-), 2.56–2.65 (1H, m, -CH- of DACH), 2.54 (3H, s, -N(CH₃)₂), 2.50 (1H, m, -CH₂- of DACH), 2.39–2.47 (1H, m, -CH- of DACH), 1.91 (3H, s, -N(CH₃)₂), 1.82 (2H, m, -CH₂- of DACH), 1.36–1.47 (12H, m, Ar-(CH₃)₃; O-CH₂-CH₃), 1.20–1.32 (11H, m, Ar-(CH₃)₃; -CH₂- of DACH), 1.02–1.18 (3H, m, -CH₂- of DACH). ¹³C{¹H} NMR (151 MHz, CD₂Cl₂): δ 163.1 (Ar C), 138.8 (Ar C), 136.6 (Ar C-H), 126.8 (Ar C-H), 124.5 (Ar C), 119.8 (Ar C), 67.2 (N-CH₂-Ar), 62.0 (O-CH₂-CH₃), 53.2 (N-CH-CH₂), 50.2 (N-CH-CH₂), 46.0 (N(CH₃)₂), 38.1 (N(CH₃)₂), 35.6 (Ar-C(CH₃)₃), 34.3 (Ar-C(CH₃)₃), 32.1 (Ar-C(CH₃)₃), 31.1 (Ar-C(CH₃)₃), 30.4 (-CH₂- of DACH), 25.4 (-CH₂- of DACH), 25.2 (-CH₂- of DACH), 22.7 (-CH₂- of DACH), 19.6 (O-CH₂-CH₃). Anal. Calcd for C₄₈H₈₄I₃In₂N₄O₄: C, 45.46; H, 6.64; N, 4.43. Found: C, 45.13; H, 6.64; N, 4.40.

Representative NMR Scale Polymerization with 5, 6, 7, 8, and 10. A Teflon-sealed NMR tube was charged with a 0.25 mL solution of a catalyst stock solution (0.25 mL, **5**, **6**, **7**, **10**, 0.0091 M, 0.0023 mmol; **8**, 0.00228 M, 0.00057 mmol) in CDCl₃ and made up to 0.5 mL with a 0.25 mL solution of CDCl₃, and the solution was mixed and frozen in a glovebox using a liquid N₂ cold wall. A stock solution of *rac*-lactide (0.91 M, 0.46 mmol for **5**, **6**, **7**, **10**; 0.228 M, 0.114 mmol for **8**) and an internal standard 1,3,5-trimethoxybenzene (5 mg, 0.03 mmol for **5**, **6**, **7**, **10**; 1.2 mg, 0.0075 mmol for **8**) in 0.5 mL of CDCl₃ were added to the frozen complex solution and frozen again, forming a bilayer. The NMR tube was sealed and quickly evacuated by vacuum to remove N₂ gas from the NMR tube. Two solutions were thawed and quickly mixed before the NMR tube was loaded into the NMR spectrometer (400 MHz Avance Bruker spectrometer). The polymerization was monitored to 90% conversion.

Representative Large-Scale Polymerization with Complex 5. A 20 mL scintillation vial was charged with a solution of complex **5** (1.0 mg, 0.00091 mmol) in 2 mL of CH₂Cl₂. A solution of *rac*-lactide (131 mg, 0.91 mmol) in 2 mL of CH₂Cl₂ was added dropwise to the vial. The resulting mixture was stirred at room temperature for 16 h. The resulting clear solution was concentrated to dryness. A sample of the residue was dissolved in CDCl₃ to be analyzed by ¹H NMR spectroscopy to determine conversion. The remaining polymeric material was dissolved in a minimum amount of CH₂Cl₂ (1 mL) and added to cold wet methanol (0 °C, 7 mL). The polymer precipitated from solution and was isolated by centrifugation. The supernatant was decanted, and the polymer was dried under high vacuum for 2 h prior to analysis.

Procedure for in Situ Crossover between 3 and 5. ¹H NMR spectroscopy (400 MHz NMR spectrometer, CD₂Cl₂ at room temperature) was used to monitor the crossover of complexes **3** and **5**. In a glovebox, a solution of complex **3** (0.5 mL, 0.0045 M) was loaded to a Teflon-sealed NMR tube and frozen in a liquid N₂ cold well (-90 °C). A solution of complex **5** (0.5 mL, 0.0046 M) was added to the frozen solution of complex **3** and frozen again, forming a bilayer. Two solutions were thawed and quickly mixed before the NMR tube was loaded into the NMR spectrometer.

Procedure for in Situ Crossover between (R,R/R,R)- and (S,S/S,S)-8. ¹H NMR spectroscopy (400 MHz NMR spectrometer, CDCl₃ at room temperature) was used to monitor the crossover of (R,R/R,R)- and (S,S/S,S)-**8**. In a glovebox, a solution of (R,R/R,R)-**8** (0.5 mL, 0.62 mM) was loaded into a Teflon-sealed NMR tube and frozen in a liquid N₂ cold well (-90 °C). A solution of (S,S/S,S)-**8** (0.5 mL, 0.62 mM) was added to the frozen solution of (R,R/R,R)-**8** and frozen again, forming a bilayer. Two solutions were thawed and quickly mixed before the NMR tube was loaded into the NMR spectrometer.

Procedure for in Situ Reactivity of (\pm)-5 with 2 equiv of Pyridine, Ethyl Acetate, Water, and Ethanol. ^1H NMR spectroscopy (400 MHz NMR spectrometer, CDCl_3 at room temperature) was used to monitor the reactivity of (\pm)-5 with pyridine, ethyl acetate, water, and ethanol. In a glovebox, a solution of complex 5 (0.25 mL, 0.0023 M) was loaded into a Teflon-sealed NMR tube and made up to 0.5 mL with a 0.25 mL solution of CDCl_3 . The solution was mixed and frozen in the glovebox using a liquid N_2 cold wall (-90°C). A solution of pyridine (0.5 mL, 0.0046 M) was added to the frozen solution of (\pm)-5 and frozen again, forming a bilayer. The solutions were thawed and quickly mixed before the NMR tube was loaded into the NMR spectrometer.

Procedure for in Situ Reactivity of (\pm)-5 with 10 equiv of Pyridine. ^1H NMR spectroscopy ((400 MHz NMR spectrometer), CD_2Cl_2 at variable temperatures (300–180 K)) was calibrated by 4% methanol in methanol- d_4 prior to each sample measurement. In a glovebox, a solution of complex 5 (0.5 mL, 0.0023 M) was loaded into a Teflon-sealed NMR tube and made up to 0.5 mL with a 0.25 mL solution of CD_2Cl_2 , and a solution of pyridine (0.5 mL, 0.023 M) was added to the solution of (\pm)-5. The solutions were mixed at room temperature, and the NMR tube was loaded into the NMR spectrometer.

Procedure for Reactivity of (\pm)-5 with Neat Methanol, Isopropanol, and Pyridine. A 20 mL scintillation vial was charged with (\pm)-5 (5.0 mg, 0.0045 mmol), and approximately 5 mL of alcohol was added to the vial. The mixture was stirred for 16 h at room temperature. The solvent was removed under vacuum, and the resulting white solid was washed with hexane and further dried in vacuo for a few hours prior to analysis by ^1H NMR spectroscopy.

Representative Sample Preparation with (\pm)-5 for PGSE NMR Studies. Each sample of (\pm)-(NNO_{tBu})H (1.4 mg, 0.0045 M), (\pm)-1 (2.4 mg, 0.0045 M), (\pm)-(NNO_{tBu})InMe₂ (2.3 mg, 0.0045 M), and (\pm)-5 (5 mg, 0.0045 M) was made up with a solution of tetrakis(trimethylsilyl)silane (TMSS) (0.94 mM, CD_2Cl_2) also used as internal standard. Because of the low solubility of (*meso*)-8 in CD_2Cl_2 , a saturated solution was made up with a solution of tetrakis(trimethylsilyl)silane (0.94 mM, CD_2Cl_2).

Representative Large-Scale Polymerization of *rac*-Lactide Using Mixtures of 5 and 1. A 20 mL scintillation vial was charged with a solution of *rac*-lactide (129.3 mg, 0.92 mmol) in 3 mL of CH_2Cl_2 . A solution consisting of complex 5 (5 mg, 0.0046 mmol) and 1 (2.5 mg, 0.0046 mmol) in 2 mL of CH_2Cl_2 was added to the vial, and the resulting mixture was stirred at room temperature for 16 h. The resulting clear solution was concentrated to dryness. A sample of the residue was dissolved in CDCl_3 to be analyzed by ^1H NMR spectroscopy to determine conversion. The remaining polymeric material was dissolved in a minimum amount of CH_2Cl_2 (1 mL) and added to cold wet methanol (0°C , 7 mL). The polymer precipitated from solution and was isolated by centrifugation. The supernatant was decanted, and the polymer was dried under high vacuum for 2 h prior to analysis.

Representative Polymerization for Variable Conversions of *rac*-LA with (*R,R,R,R*)-5 at 0°C . A Schlenk flask (a bomb flask) was charged with a 0.25 mL solution of a catalyst stock solution (0.25 mL, 5: 0.0032 M, 0.0008 mmol) in CH_2Cl_2 and made up to 0.5 mL with a 0.25 mL solution of CH_2Cl_2 , and the solution was mixed and frozen in the glovebox using a liquid N_2 cold wall. A stock solution of *rac*-lactide (0.32 M, 0.398 mmol) in 1.25 mL of CH_2Cl_2 was added to the frozen complex solution and frozen again, forming a bilayer. The Schlenk flask was sealed, and two solutions were thawed and quickly mixed before the flask was immersed into an ice bath to maintain the reaction temperature at 0°C . At a certain time, the resulting clear solution was concentrated to dryness. A 1 mL solution of HCl (1.5 M HCl in Et_2O) was added to the reaction mixture to quench the polymerization and removed under vacuum. The sample of the residue was dissolved in CDCl_3 to be analyzed by ^1H NMR spectroscopy (600 MHz) to determine conversion and tacticity of the resulting polymer.

■ ASSOCIATED CONTENT

📄 Supporting Information

Full solid-state and solution characterization of complexes as well as kinetics and stereoselectivity studies of polymerization (Figures S1–S50). This material is available free of charge via the Internet at <http://pubs.acs.org>.

■ AUTHOR INFORMATION

Corresponding Author

mehr@chem.ubc.ca

Notes

The authors declare no competing financial interest.

■ ACKNOWLEDGMENTS

We thank UBC, NSERC, CFI, and BCKDF for funding, C. C. Yan, T. Janes, K. Rebullar, and S. Bishop for the synthesis of starting materials, and Dr. M. Ezhova for her technical assistance with the NMR spectroscopy. I.Y. acknowledges Brian Patrick for valuable discussions on solving some structures.

■ REFERENCES

- (a) Drumright, R. E.; Gruber, P. R.; Henton, D. E. *Adv. Mater.* **2000**, *12*, 1841–1846. (b) Mecking, S. *Angew. Chem., Int. Ed.* **2004**, *43*, 1078–1085.
- (a) Gupta, A. P.; Kumar, V. *Eur. Polym. J.* **2007**, *43*, 4053–4074. (b) Gupta, B.; Revagade, N.; Hilborn, J. *Prog. Polym. Sci.* **2007**, *32*, 455–482. (c) Thomas, C. M.; Lutz, J.-F. *Angew. Chem., Int. Ed.* **2011**, *50*, 9244–9246.
- (a) Kamber, N. E.; Jeong, W.; Waymouth, R. M.; Pratt, R. C.; Lohmeijer, B. G. G.; Hedrick, J. L. *Chem. Rev.* **2007**, *107*, 5813–5840. (b) Castillo, J. A.; Borchmann, D. E.; Cheng, A. Y.; Wang, Y. F.; Hu, C.; Garcia, A. J.; Weck, M. *Macromolecules* **2012**, *45*, 62–69. (c) Coulembier, O.; Lemaure, V.; Josse, T.; Minoia, A.; Cornil, J.; Dubois, P. *Chem. Sci.* **2012**, *3*, 723–726. (d) Sen, T. K.; Sau, S. C.; Mukherjee, A.; Modak, A.; Mandal, S. K.; Koley, D. *Chem. Commun.* **2011**, *47*, 11972–11974. (e) Qian, H. T.; Wohl, A. R.; Crow, J. T.; Macosko, C. W.; Hoye, T. R. *Macromolecules* **2011**, *44*, 7132–7140. (f) Makiguchi, K.; Satoh, T.; Kakuchi, T. *J. Polym. Sci., Part A: Polym. Chem.* **2011**, *49*, 3769–3777. (g) Makiguchi, K.; Satoh, T.; Kakuchi, T. *Macromolecules* **2011**, *44*, 1999–2005. (h) Miyake, G. M.; Chen, E. Y. X. *Macromolecules* **2011**, *44*, 4116–4124. (i) Kakuchi, R.; Tsuji, Y.; Chiba, K.; Fuchise, K.; Sakai, R.; Satoh, T.; Kakuchi, T. *Macromolecules* **2010**, *43*, 7090–7094. (j) Koeller, S.; Kadota, J.; Deffieux, A.; Peruch, F.; Massip, S.; Leger, J. M.; Desvergne, J. P.; Bibal, B. *J. Am. Chem. Soc.* **2009**, *131*, 15088–15089. (k) Zhang, L.; Nederberg, F.; Pratt, R. C.; Waymouth, R. M.; Hedrick, J. L.; Wade, C. G. *Macromolecules* **2007**, *40*, 4154–4158. (l) Culkin, D. A.; Jeong, W. H.; Csihony, S.; Gomez, E. D.; Balsara, N. R.; Hedrick, J. L.; Waymouth, R. M. *Angew. Chem., Int. Ed.* **2007**, *46*, 2627–2630. (m) Dove, A. P.; Li, H. B.; Pratt, R. C.; Lohmeijer, B. G. G.; Culkin, D. A.; Waymouth, R. M.; Hedrick, J. L. *Chem. Commun.* **2006**, 2881–2883. (n) Pratt, R. C.; Lohmeijer, B. G. G.; Long, D. A.; Lundberg, P. N. P.; Dove, A. P.; Li, H. B.; Wade, C. G.; Waymouth, R. M.; Hedrick, J. L. *Macromolecules* **2006**, *39*, 7863–7871. (o) Pratt, R. C.; Lohmeijer, B. G. G.; Long, D. A.; Waymouth, R. M.; Hedrick, J. L. *J. Am. Chem. Soc.* **2006**, *128*, 4556–4557.
- (a) Williams, C. K.; Hillmyer, M. A. *Polym. Rev.* **2008**, *48*, 1–10. (b) Chivers, T.; Konu, J. *Comments Inorg. Chem.* **2009**, *30*, 131–176. (c) Williams, C. K. *Chem. Soc. Rev.* **2007**, *36*, 1573–1580. (d) Hoogenboom, R.; Schubert, U. S. *Chem. Soc. Rev.* **2006**, *35*, 622–629.
- (a) Dijkstra, P. J.; Du, H. Z.; Feijen, J. *Polym. Chem.* **2011**, *2*, 520–527. (b) Buffet, J. C.; Okuda, J. *Polym. Chem.* **2011**, *2*, 2758–2763. (c) Thomas, C. M. *Chem. Soc. Rev.* **2010**, *39*, 165–173. (d) Stanford, M. J.; Dove, A. P. *Chem. Soc. Rev.* **2010**, *39*, 486–494. (e) Dechy-Cabaret, O.; Martin-Vaca, B.; Bourissou, D. *Chem. Rev.*

- 2004, 104, 6147–6176. (f) O'Keefe, B. J.; Hillmyer, M. A.; Tolman, W. B. *J. Chem. Soc., Dalton Trans.* **2001**, 2215–2224.
- (6) (a) Sutar, A. K.; Maharana, T.; Dutta, S.; Chen, C. T.; Lin, C. C. *Chem. Soc. Rev.* **2010**, 39, 1724–1746. (b) Lu, W. Y.; Hsiao, M. W.; Hsu, S. C. N.; Peng, W. T.; Chang, Y. J.; Tsou, Y. C.; Wu, T. Y.; Lai, Y. C.; Chen, Y.; Chen, H. Y. *Dalton Trans.* **2012**, 41, 3659–3667. (c) Huang, Y.; Tsai, Y. H.; Hung, W. C.; Lin, C. S.; Wang, W.; Huang, J. H.; Dutta, S.; Lin, C. C. *Inorg. Chem.* **2010**, 49, 9416–9425. (d) Yu, T. L.; Huang, B. H.; Hung, W. C.; Lin, C. C.; Wang, T. C.; Ho, R. M. *Polymer* **2007**, 48, 4401–4411. (e) Huang, C. A.; Chen, C. T. *Dalton Trans.* **2007**, 5561–5566. (f) Hsueh, M. L.; Huang, B. H.; Wu, J. C.; Lin, C. C. *Macromolecules* **2005**, 38, 9482–9487. (g) Ko, B. T.; Lin, C. C. *J. Am. Chem. Soc.* **2001**, 123, 7973–7977.
- (7) (a) Cushion, M. G.; Mountford, P. *Chem. Commun.* **2011**, 47, 2276–2278. (b) Sarazin, Y.; Liu, B.; Roisnel, T.; Maron, L.; Carpentier, J. F. *J. Am. Chem. Soc.* **2011**, 133, 9069–9087. (c) Wheaton, C. A.; Hayes, P. G. *Catal. Sci. Technol.* **2012**, 2, 125–138. (d) Sung, C. Y.; Li, C. Y.; Su, J. K.; Chen, T. Y.; Lin, C. H.; Ko, B. T. *Dalton Trans.* **2012**, 41, 953–961. (e) Song, S. D.; Zhang, X. Y.; Ma, H. Y.; Yang, Y. *Dalton Trans.* **2012**, 41, 3266–3277. (f) Sun, H. S.; Ritch, J. S.; Hayes, P. G. *Inorg. Chem.* **2011**, 50, 8063–8072. (g) Ma, W. A.; Wang, Z. X. *Organometallics* **2011**, 30, 4364–4373. (h) Grala, A.; Eijfler, J.; Jerzykiewicz, L. B.; Sobota, P. *Dalton Trans.* **2011**, 40, 4042–4044. (i) Chuang, H. J.; Weng, S. F.; Chang, C. C.; Lin, C. C.; Chen, H. Y. *Dalton Trans.* **2011**, 40, 9601–9607. (j) Chen, H. Y.; Peng, Y. L.; Huang, T. H.; Sutar, A. K.; Miller, S. A.; Lin, C. C. *J. Mol. Catal. A: Chem.* **2011**, 339, 61–71. (k) Borner, J.; Vieira, I. D.; Pawlis, A.; Doring, A.; Kuckling, D.; Herres-Pawlis, S. *Chem.-Eur. J.* **2011**, 17, 4507–4512. (l) Wheaton, C. A.; Hayes, P. G. *Chem. Commun.* **2010**, 46, 8404–8406. (m) Wang, L. Y.; Ma, H. Y. *Dalton Trans.* **2010**, 39, 7897–7910. (n) Wang, L. Y.; Ma, H. Y. *Macromolecules* **2010**, 43, 6535–6537. (o) Liu, Z. Z.; Gao, W.; Zhang, J. S.; Cui, D. M.; Wu, Q. L.; Mu, Y. *Organometallics* **2010**, 29, 5783–5790. (p) Drouin, F.; Oguadinma, P. O.; Whitehorne, T. J. J.; Prud'homme, R. E.; Schaper, F. *Organometallics* **2010**, 29, 2139–2147. (q) Di Iulio, C.; Jones, M. D.; Mahon, M. F.; Apperley, D. C. *Inorg. Chem.* **2010**, 49, 10232–10234. (r) Darensbourg, D. J.; Karroonnirun, O. *Macromolecules* **2010**, 43, 8880–8886. (s) Wheaton, C. A.; Ireland, B. J.; Hayes, P. G. *Organometallics* **2009**, 28, 1282–1285. (t) Tsai, Y. H.; Lin, C. H.; Lin, C. C.; Ko, B. T. *J. Polym. Sci., Part A: Polym. Chem.* **2009**, 47, 4927–4936. (u) Shen, M. Y.; Peng, Y. L.; Hung, W. C.; Lin, C. C. *Dalton Trans.* **2009**, 9906–9913. (v) Labourdette, G.; Lee, D. J.; Patrick, B. O.; Ezhova, M. B.; Mehrkhodavandi, P. *Organometallics* **2009**, 28, 1309–1319. (w) Grunova, E.; Roisnel, T.; Carpentier, J. F. *Dalton Trans.* **2009**, 9010–9019. (x) Chen, M. T.; Chang, P. J.; Huang, C. A.; Peng, K. F.; Chen, C. T. *Dalton Trans.* **2009**, 9068–9074. (y) Arnold, P. L.; Casely, I. J.; Turner, Z. R.; Bellabarba, R.; Tooze, R. B. *Dalton Trans.* **2009**, 7236–7247. (z) Wu, J. C.; Chen, Y. Z.; Hung, W. C.; Lin, C. C. *Organometallics* **2008**, 27, 4970–4978. (aa) Eijfler, J.; Szafert, S.; Mierzwicki, K.; Jerzykiewicz, L. B.; Sobota, P. *Dalton Trans.* **2008**, 6556–6562. (bb) Tang, H. Y.; Chen, H. Y.; Huang, J. H.; Lin, C. C. *Macromolecules* **2007**, 40, 8855–8860. (cc) Lian, B.; Thomas, C. M.; Casagrande, O. L.; Lehmann, C. W.; Roisnel, T.; Carpentier, J. F. *Inorg. Chem.* **2007**, 46, 328–340. (dd) Chisholm, M. H.; Gallucci, J. C.; Phomphrai, K. *Inorg. Chem.* **2005**, 44, 8004–8010. (ee) Chisholm, M. H.; Lin, C. C.; Gallucci, J. C.; Ko, B. T. *Dalton Trans.* **2003**, 406–412. (ff) Chisholm, M. H.; Gallucci, J.; Phomphrai, K. *Chem. Commun.* **2003**, 48–49.
- (8) (a) Matsubara, K.; Terata, C.; Sekine, H.; Yamatani, K.; Harada, T.; Eda, K.; Dan, M.; Koga, Y.; Yasuniwa, M. *J. Polym. Sci., Part A: Polym. Chem.* **2012**, 50, 957–966. (b) Chen, H. L.; Dutta, S.; Huang, P. Y.; Lin, C. C. *Organometallics* **2012**, 31, 2016–2025. (c) Whitelaw, E. L.; Loraine, G.; Mahon, M. F.; Jones, M. D. *Dalton Trans.* **2011**, 40, 11469–11473. (d) Qian, F.; Liu, K. Y.; Ma, H. Y. *Chin. J. Catal.* **2011**, 32, 189–196. (e) Otero, A.; Lara-Sanchez, A.; Fernandez-Baeza, J.; Alonso-Moreno, C.; Castro-Osma, J. A.; Marquez-Segovia, I.; Sanchez-Barba, L. F.; Rodriguez, A. M.; Garcia-Martinez, J. C. *Organometallics* **2011**, 30, 1507–1522. (f) Li, C. Y.; Tsai, C. Y.; Lin, C. H.; Ko, B. T. *Dalton Trans.* **2011**, 40, 1880–1887. (g) Darensbourg, D. J.; Karroonnirun, O.; Wilson, S. J. *Inorg. Chem.* **2011**, 50, 6775–6787. (h) Thibault, M. H.; Fontaine, F. G. *Dalton Trans.* **2010**, 39, 5688–5697. (i) Silvestri, A.; Grisi, F.; Milione, S. *J. Polym. Sci., Part A: Polym. Chem.* **2010**, 48, 3632–3639. (j) Schwarz, A. D.; Chu, Z. Y.; Mountford, P. *Organometallics* **2010**, 29, 1246–1260. (k) Qian, F.; Liu, K. Y.; Ma, H. Y. *Dalton Trans.* **2010**, 39, 8071–8083. (l) Phomphrai, K.; Chumsaeng, P.; Sangtrirutnugul, P.; Kongsaree, P.; Pohmakotr, M. *Dalton Trans.* **2010**, 39, 1865–1871. (m) Hild, F.; Haquette, P.; Brelot, L.; Dagorne, S. *Dalton Trans.* **2010**, 39, 533–540. (n) Bouyahyi, M.; Roisnel, T.; Carpentier, J. F. *Organometallics* **2010**, 29, 491–500. (o) Du, H. Z.; Velders, A. H.; Dijkstra, P. J.; Sun, J. R.; Zhong, Z. Y.; Chen, X. S.; Feijen, J. *Chem.-Eur. J.* **2009**, 15, 9836–9845. (p) Chisholm, M. H.; Gallucci, J. C.; Quisenberry, K. T.; Zhou, Z. P. *Inorg. Chem.* **2008**, 47, 2613–2624. (q) Bouyahyi, M.; Grunova, E.; Marquet, N.; Kirillov, E.; Thomas, C. M.; Roisnel, T.; Carpentier, J. F. *Organometallics* **2008**, 27, 5815–5825. (r) Nomura, N.; Ishii, R.; Yamamoto, Y.; Kondo, T. *Chem.-Eur. J.* **2007**, 13, 4433–4451. (s) Du, H. Z.; Pang, X.; Yu, H. Y.; Zhuang, X. L.; Chen, X. S.; Cui, D. M.; Wang, X. H.; Jing, X. B. *Macromolecules* **2007**, 40, 1904–1913. (t) Ma, H. Y.; Melillo, G.; Oliva, L.; Spaniol, T. P.; Englert, U.; Okuda, J. *Dalton Trans.* **2005**, 721–727. (u) Chisholm, M. H.; Patmore, N. J.; Zhou, Z. P. *Chem. Commun.* **2005**, 127–129. (v) Amgoune, A.; Lavanant, L.; Thomas, C. M.; Chi, Y.; Welter, R.; Dagorne, S.; Carpentier, J. F. *Organometallics* **2005**, 24, 6279–6282. (w) Tang, Z. H.; Chen, X. S.; Yang, Y. K.; Pang, X.; Sun, J. R.; Zhang, X. F.; Jing, X. B. *J. Polym. Sci., Part A: Polym. Chem.* **2004**, 42, 5974–5982. (x) Ishii, R.; Nomura, N.; Kondo, T. *Polym. J.* **2004**, 36, 261–264. (y) Hormnirun, P.; Marshall, E. L.; Gibson, V. C.; White, A. J. P.; Williams, D. J. *J. Am. Chem. Soc.* **2004**, 126, 2688–2689.
- (9) (a) Nomura, N.; Ishii, R.; Akakura, M.; Aoi, K. *J. Am. Chem. Soc.* **2002**, 124, 5938–5939. (b) Zhong, Z. Y.; Dijkstra, P. J.; Feijen, J. *J. Am. Chem. Soc.* **2003**, 125, 11291–11298. (c) Zhong, Z. Y.; Dijkstra, P. J.; Feijen, J. *Angew. Chem., Int. Ed.* **2002**, 41, 4510–4513. (d) Ovitt, T. M.; Coates, G. W. *J. Am. Chem. Soc.* **2002**, 124, 1316–1326. (e) Ovitt, T. M.; Coates, G. W. *J. Polym. Sci., Part A: Polym. Chem.* **2000**, 38, 4686–4692. (f) Spassky, N.; Wisniewski, M.; Pluta, C.; LeBorgne, A. *Macromol. Chem. Phys.* **1996**, 197, 2627–2637. (g) Le Borgne, A.; Vincens, V.; Jouglard, M.; Spassky, N. *Makromol. Chem., Macromol. Symp.* **1993**, 73, 37–46.
- (10) Horeglad, P.; Kruk, P.; Pecaut, J. *Organometallics* **2010**, 29, 3729–3734.
- (11) Chmura, A. J.; Chuck, C. J.; Davidson, M. G.; Jones, M. D.; Lunn, M. D.; Bull, S. D.; Mahon, M. F. *Angew. Chem., Int. Ed.* **2007**, 46, 2280–2283.
- (12) (a) Nimitsiriwat, N.; Gibson, V. C.; Marshall, E. L.; Elsegood, M. R. *J. Dalton Trans.* **2009**, 3710–3715. (b) Nimitsiriwat, N.; Gibson, V. C.; Marshall, E. L.; Elsegood, M. R. *J. Inorg. Chem.* **2008**, 47, 5417–5424. (c) Dove, A. P.; Gibson, V. C.; Marshall, E. L.; Rzepa, H. S.; White, A. J. P.; Williams, D. J. *J. Am. Chem. Soc.* **2006**, 128, 9834–9843. (d) Kowalski, A.; Libiszowski, J.; Biela, T.; Cypriak, M.; Duda, A.; Penczek, S. *Macromolecules* **2005**, 38, 8170–8176. (e) Nimitsiriwat, N.; Marshall, E. L.; Gibson, V. C.; Elsegood, M. R. J.; Dale, S. H. *J. Am. Chem. Soc.* **2004**, 126, 13598–13599. (f) Lahcini, M.; Castro, P. M.; Kalmi, M.; Leskela, M.; Repo, T. *Organometallics* **2004**, 23, 4547–4549. (g) Chisholm, M. H.; Delbridge, E. E.; Gallucci, J. C. *New J. Chem.* **2004**, 28, 145–152. (h) Dove, A. P.; Gibson, V. C.; Marshall, E. L.; White, A. J. P.; Williams, D. J. *Chem. Commun.* **2001**, 283–284.
- (13) Kricheldorf, H. R. *Chem. Rev.* **2009**, 109, 5579–5594.
- (14) (a) Gorczynski, J. L.; Chen, J. B.; Fraser, C. L. *J. Am. Chem. Soc.* **2005**, 127, 14956–14957. (b) McGuinness, D. S.; Marshall, E. L.; Gibson, V. C.; Steed, J. W. *J. Polym. Sci., Part A: Polym. Chem.* **2003**, 41, 3798–3803. (c) Gibson, V. C.; Marshall, E. L.; Navarro-Llobet, D.; White, A. J. P.; Williams, D. J. *J. Chem. Soc., Dalton Trans.* **2002**, 4321–4322.
- (15) (a) Stopper, A.; Okuda, J.; Kol, M. *Macromolecules* **2012**, 45, 698–704. (b) Jeffery, B. J.; Whitelaw, E. L.; Garcia-Vivo, D.; Stewart, J. A.; Mahon, M. F.; Davidson, M. G.; Jones, M. D. *Chem. Commun.* **2011**, 47, 12328–12330. (c) Buffet, J.-C.; Okuda, J. *Chem. Commun.* **2011**, 47, 4796–4798. (d) Whitelaw, E. L.; Jones, M. D.; Mahon, M. F.

- Inorg. Chem.* **2010**, *49*, 7176–7181. (e) Schwarz, A. D.; Herbert, K. R.; Paniagua, C.; Mountford, P. *Organometallics* **2010**, *29*, 4171–4188. (f) Saha, T. K.; Rajashekar, B.; Gowda, R. R.; Ramkumar, V.; Chakraborty, D. *Dalton Trans.* **2010**, *39*, 5091–5093. (g) Zelikoff, A. L.; Kopilov, J.; Goldberg, I.; Coates, G. W.; Kol, M. *Chem. Commun.* **2009**, 6804–6806. (h) Ning, Y.; Zhang, Y.; Rodriguez-Delgado, A.; Chen, E. Y. X. *Organometallics* **2008**, *27*, 5632–5640. (i) Chmura, A. J.; Davidson, M. G.; Frankis, C. J.; Jones, M. D.; Lunn, M. D. *Chem. Commun.* **2008**, 6611–6611. (j) Chmura, A. J.; Davidson, M. G.; Frankis, C. J.; Jones, M. D.; Lunn, M. D. *Chem. Commun.* **2008**, 1293–1295. (k) Gornshstein, F.; Kapon, M.; Botoshansky, M.; Eisen, M. S. *Organometallics* **2007**, *26*, 497–507. (l) Atkinson, R. C. J.; Gerry, K.; Gibson, V. C.; Long, N. J.; Marshall, E. L.; West, L. J. *Organometallics* **2007**, *26*, 316–320. (m) Chmura, A. J.; Davidson, M. G.; Jones, M. D.; Lunn, M. D.; Mahon, M. F.; Johnson, A. F.; Khunkamchoo, P.; Roberts, S. L.; Wong, S. S. F. *Macromolecules* **2006**, *39*, 7250–7257. (n) Amgoune, A.; Thomas, C. M.; Roisnel, T.; Carpentier, J. F. *Chem.-Eur. J.* **2006**, *12*, 169–179.
- (16) (a) Otero, A.; Fernandez-Baeza, J.; Lara-Sanchez, A.; Alonso-Moreno, C.; Marquez-Segovia, I.; Sanchez-Barba, L. F.; Rodriguez, A. M. *Angew. Chem., Int. Ed.* **2009**, *48*, 2176–2179. (b) Platel, R. H.; White, A. J. P.; Williams, C. K. *Inorg. Chem.* **2011**, *50*, 7718–7728. (c) Broderick, E. M.; Guo, N.; Wu, T. P.; Vogel, C. S.; Xu, C. L.; Sutter, J.; Miller, J. T.; Meyer, K.; Cantat, T.; Diaconescu, P. L. *Chem. Commun.* **2011**, 47, 9897–9899. (d) Broderick, E. M.; Guo, N.; Vogel, C. S.; Xu, C.; Sutter, J.; Miller, J. T.; Meyer, K.; Mehrkhodavandi, P.; Diaconescu, P. L. *J. Am. Chem. Soc.* **2011**, *133*, 9278–9281. (e) Wong, A. W.; Miller, K. L.; Diaconescu, P. L. *Dalton Trans.* **2010**, *39*, 6726–6731. (f) Diaconescu, P. L. *Comments Inorg. Chem.* **2010**, *31*, 196–241. (g) Platel, R. H.; White, A. J. P.; Williams, C. K. *Chem. Commun.* **2009**, 4115–4117. (h) Stanlake, L. J. E.; Beard, J. D.; Schafer, L. L. *Inorg. Chem.* **2008**, *47*, 8062–8068. (i) Platel, R. H.; White, A. J. P.; Williams, C. K. *Inorg. Chem.* **2008**, *47*, 6840–6849. (j) Hodgson, L. M.; Platel, R. H.; White, A. J. P.; Williams, C. K. *Macromolecules* **2008**, *41*, 8603–8607. (k) Carver, C. T.; Monreal, M. J.; Diaconescu, P. L. *Organometallics* **2008**, *27*, 363–370. (l) Wheaton, C. A.; Hayes, P. G.; Ireland, B. J. *Dalton Trans.* **2009**, 4832–4846.
- (17) Douglas, A. F.; Patrick, B. O.; Mehrkhodavandi, P. *Angew. Chem., Int. Ed.* **2008**, *47*, 2290–2293.
- (18) An indium complex for the polymerization of caprolactone has also been reported: Hsieh, I. P.; Huang, C. H.; Lee, H. M.; Kuo, P. C.; Huang, J. H.; Lee, H. I.; Cheng, J. T.; Lee, G. H. *Inorg. Chim. Acta* **2006**, *359*, 497–504.
- (19) (a) Acosta-Ramirez, A.; Douglas, A. F.; Yu, I.; Patrick, B. O.; Diaconescu, P. L.; Mehrkhodavandi, P. *Inorg. Chem.* **2010**, *49*, 5444–5452. (b) Osten, K.; Yu, I.; Duffy, I. R.; Lagaditis, P. V. O.; Yu, C.-C.; Wallis, C. J.; Mehrkhodavandi, P. *Dalton Trans.* **2012**, *41*, 8123–8134. (c) Ul-haq, M. I.; Acosta-Ramirez, A.; Mehrkhodavandi, P.; Signorell, R. J. *Supercrit. Fluids* **2010**, *51*, 376–383. (d) Othman, N.; Acosta-Ramirez, A.; Mehrkhodavandi, P.; Dorgan, J. R.; Hatzikiriakos, S. G. *J. Rheol.* **2011**, *55*, 987–1005. (e) Othman, N.; Jazrawi, B.; Mehrkhodavandi, P.; Hatzikiriakos, S. G. *Rheol. Acta* **2012**, *51*, 357–369. (f) Othman, N.; Xu, C.; Mehrkhodavandi, P.; Hatzikiriakos, S. G. *Polymer* **2012**, *53*, 2443–2452. (g) Xu, C.; Yu, I.; Mehrkhodavandi, P. *Chem. Commun.* **2012**, 48, 6806–6808.
- (20) (a) Buffet, J.-C.; Okuda, J.; Arnold, P. L. *Inorg. Chem.* **2010**, *49*, 419–426. (b) Peckermann, I.; Kapelski, A.; Spaniol, T. P.; Okuda, J. *Inorg. Chem.* **2009**, *48*, 5526–5534. (c) Hu, M. G.; Wang, M.; Zhang, P. L.; Wang, L.; Zhu, F. J.; Sun, L. C. *Inorg. Chem. Commun.* **2010**, *13*, 968–971. (d) Blake, M. P.; Schwarz, A. D.; Mountford, P. *Organometallics* **2011**, *30*, 1202–1214. (e) Normand, M.; Kirillov, E.; Roisnel, T.; Carpentier, J. F. *Organometallics* **2012**, *31*, 1448–1457.
- (21) (a) Pietrangelo, A.; Hillmyer, M. A.; Tolman, W. B. *Chem. Commun.* **2009**, 2736–2737. (b) Pietrangelo, A.; Knight, S. C.; Gupta, A. K.; Yao, L. J.; Hillmyer, M. A.; Tolman, W. B. *J. Am. Chem. Soc.* **2010**, *132*, 11649–11657.
- (22) O’Keefe, B. J.; Breyfogle, L. E.; Hillmyer, M. A.; Tolman, W. B. *J. Am. Chem. Soc.* **2002**, *124*, 4384–4393.
- (23) O’Keefe, B. J.; Monnier, S. M.; Hillmyer, M. A.; Tolman, W. B. *J. Am. Chem. Soc.* **2001**, *123*, 339–340.
- (24) Williams, C. K.; Breyfogle, L. E.; Choi, S. K.; Nam, W.; Young, V. G.; Hillmyer, M. A.; Tolman, W. B. *J. Am. Chem. Soc.* **2003**, *125*, 11350–11359.
- (25) Chamberlain, B. M.; Cheng, M.; Moore, D. R.; Ovitt, T. M.; Lobkovsky, E. B.; Coates, G. W. *J. Am. Chem. Soc.* **2001**, *123*, 3229–3238.
- (26) Williams, C. K.; Brooks, N. R.; Hillmyer, M. A.; Tolman, W. B. *Chem. Commun.* **2002**, 2132–2133.
- (27) Platel, R. H.; Hodgson, L. M.; White, A. J. P.; Williams, C. K. *Organometallics* **2007**, *26*, 4955–4963.
- (28) Ma, H. Y.; Spaniol, T. P.; Okuda, J. *Angew. Chem., Int. Ed.* **2006**, *45*, 7818–7821.
- (29) Duda, A.; Penczek, S. *Makromol. Chem., Macromol. Symp.* **1991**, *47*, 127–140.
- (30) Ma, H. Y.; Okuda, J. *Macromolecules* **2005**, *38*, 2665–2673.
- (31) Mitchell, J. M.; Finney, N. S. *Tet. Lett.* **2000**, *41*, 8431–8434.
- (32) Unlike the chloro analogues, synthetic routes involving reaction of complex **4** with NaOEt always resulted in a mixture of **7** and **8**, which can be readily separated with a 1:1 solution of acetonitrile and THF. Alternatively, KOEt can be used to generate complex **8** as a major product.
- (33) Macchioni, A.; Ciancaleoni, G.; Zuccaccia, C.; Zuccaccia, D. *Chem. Soc. Rev.* **2008**, *37*, 479–489.
- (34) Polymerization rate = $k_{\text{obs}} \times [\text{LA}]$; $k_{\text{obs}} = k[\text{cat}]$, where k is the rate constant used in the Eyring equation to derive activation parameters. Because of solubility constraints, different $[\text{cat}]$ values were used for **7** and **8**.
- (35) Coleman, M. M.; Painter, P. C. *Fundamentals of Polymer Science: An Introductory Text*, 2nd ed.; CRC Press LLC: Boca Raton, FL, 1997; pp 353–370.
- (36) Polymerization of D- and L-LA with racemic or enantiopure catalysts yields isotactic polymer; no epimerization was observed.
- (37) Girard, C.; Kagan, H. B. *Angew. Chem., Int. Ed.* **1998**, *37*, 2922–2959.
- (38) Mehrkhodavandi, P.; Yu, I.; Acosta-Ramirez, J. A. Catalysts and Methods for Cyclic Ester (Co)polymerization, and Polymer and Copolymer Products. Filing Date: May 18, 2011. Provisional Patent Application U.S. 61/487,626; CAN. 2,740,821.
- (39) Larrow, J. F.; Jacobsen, E. N.; Gao, Y.; Hong, Y. P.; Nie, X. Y.; Zepp, C. M. *J. Org. Chem.* **1994**, *59*, 1939–1942.